UNIVERSITÉ DE MONTRÉAL

DEVELOPMENT OF A TIME DELAY FORMULATION FOR FLUIDELASTIC INSTABILITY MODEL

HAO LI

DÉPARTEMENT DE GÉNIE MÉCANIQUE

ÉCOLE POLYTECHNIQUE DE MONTRÉAL

MÉMOIRE PRÉSENTÉ EN VUE DE L'OBTENTION

DU DIPLÔME DE MAÎTRISE ÈS SCIENCES APPLIQUÉES

(GÉNIE MÉCANIQUE)

AOÛT 2016

© Hao LI, 2016.

UNIVERSITÉ DE MONTRÉAL

ÉCOLE POLYTECHNIQUE DE MONTRÉAL

Ce mémoire intitulé :

DEVELOPMENT OF A TIME DELAY FORMULATION FOR FLUIDELASTIC INSTABILITY MODEL

présenté par : LI Hao

en vue de l'obtention du diplôme de : Maîtrise ès sciences appliquées

a été dûment accepté par le jury d'examen constitué de :

M. VO Huu Duc, Ph. D, président

M. MUREITHI Njuki William, Ph. D, membre et directeur de recherche

M. PETTIGREW Michel, M. Sc, membre

DEDICATION

To my parents

Jiabing Li and Lanfeng Zhang

who love me, believe in me, inspire me

and support me every step of the way

ACKNOWLEDGEMENTS

First of all, I would like to express my sincere appreciation to my supervisor, Prof. Mureithi Njuki, for offering me the opportunity to pursue my master degree in such a challenge research field, and for his constant encouragement and guidance. He has walked me through all the stages of this thesis. Without his consistent and illuminating instruction, this thesis would not have reached its present form.

Special thanks to Stephen Olala who shared his experience without reservation and illuminated the darkness of the current study with his intelligence. As well as to Farzad Ashrafi who helped me solve the problems about CFD.

Thanks to the BWC/AECL/NSERC Industrial Chair of Fluid-Structure Interaction for providing me the experimental apparatus. I would like to acknowledge each member of the Chair who supported me through their advices and encouragements, especially François de Kerret, as well as Ines Benito, Bastien Cucuel and Abdallah Hadji.

I am also indebted to Prof.Yang jianming from Southeast University for his approval of my request of studying aboard and for his continuous support and encouragement.

Many friends have helped me stay optimistic through these difficult years. Their support helped me overcome setbacks. I greatly value their friendship and I deeply appreciate their belief in me.

Finally, I must express my very profound gratitude to my family for providing me with unfailing support and continuous encouragement throughout the years of study and through the process of researching and writing this thesis.

RÉSUMÉ

Les faisceaux de tubes dans les composants industriels, tels que les échangeurs de chaleur et les générateurs de vapeur sont susceptibles d'être endommagés en raison de l'instabilité fluides-élastiques. Cette étude porte sur la modélisation de l'instabilité fluides-élastiques dans des faisceaux de tubes soumis à un écoulement transverse. Il y a consensus sur le fait d'introduire un déphasage dans les modèles d'instabilité fluides-élastiques. Bien que ce déphasage soit l'un des paramètres clés dans les modèles d'instabilité fluides-élastiques, le phénomène physique qui en est responsable est encore mal compris, et il est expliqué de manière variée.

Dans cette étude, une nouvelle formulation du déphasage pour des modèles quasi-stationnaire est dérivée dans le domaine fréquentiel sous la forme d'une fonction équivalente de Theodorsen.

Les forces fluides instationnaires et quasi-statiques ont été mesurées pour développer l'expression du déphasage. L'effet du nombre de Reynolds sur les coefficients de force statique a également été étudié. Nous avons observé que la fonction de déphasage dépend également du nombre de Reynolds, ce qui implique que l'instabilité fluides-élastiques dépend aussi du nombre de Reynolds. Des comparaisons avec les fonctions de déphasage proposées dans les modèles quasi-stationnaire et quasi-instationnaires ont été faites. Un dépassement initial de la force de portance a été observé avec le modèle actuel.

En utilisant la nouvelle expression du déphasage, l'effet du nombre de Reynolds sur l'instabilité fluides-élastiques était bien pris en considération. Une étude de stabilité a été réalisée afin de prédire la vitesse critique pour une variété de paramètres d'amortissement massique. La vitesse critique prédite pour l'instabilité fluides-élastiques a été comparée à d'autres modèles théoriques ainsi qu'à des données expérimentales de la littérature. Les résultats montrent une amélioration significative par rapport au modèle quasi-statique de déphasage constant et au modèle quasi-instationnaire. Cela confirme également la validité du modèle d'instabilité fluides-élastiques proposé et permet d'accorder de la fiabilité à la méthode.

ABSTRACT

Tube arrays in industrial components such as heat exchangers and steam generators are susceptible to damage due to fluidelastic instability (FEI). This study focuses on the modelling of fluidelastic instability in tube arrays subjected to cross-flow. There is agreement on the idea of introducing a time delay in FEI models. Although it is one of the key parameters for FEI models, the phenomenon behind this time delay is still subject to many possible explanations, and the underlying physics is still not well understood.

In the present work a new time delay formulation for the class of the quasi-steady FEI models is derived in the frequency domain in the form of an Equivalent Theodorsen Function.

Unsteady and quasi-static fluid forces were measured to develop the time delay formulation. The effect of Reynolds number on the static force coefficients was also investigated. The time delay function was found to be also dependent on the Reynolds number which implies that the fluidelastic instability is also Reynolds number dependent. Comparison to other time delay functions proposed in the quasi-steady and quasi-unsteady models is made. An initial overshoot in the lift force was observed for the present model.

Using the new time delay formulation, the effect of Reynolds number on FEI is conveniently taken into consideration. A stability analysis was carried out to predict the critical velocity for a range of mass-damping parameters. The predicted critical velocity for FEI was compared with other theoretical models and also to experiment data from the literature. The results show a significant improvement over the constant time delay quasi-steady model and the quasi-unsteady model. The results also confirm the validity of the proposed FEI model and give some confidence in the reliability of the method.

TABLE OF CONTENTS

LIST OF TABLES

LIST OF FIGURES

LIST OF SYMBOLS AND ABBREVIATIONS

$[M_s],[C_s],[K_s]$	The mass, damping and stiffness matrices of the structure, respectively
$[M_f],[C_f],[K_f]$	The added mass, damping and stiffness matrices of the fluid, respectively
$\ddot{x},\dot{x},x$	Tube acceleration, velocity, displacement vector, respectively
F_f	General form of the fluid force
ρ	Fluid density
U,U_p	Flow free stream velocity, flow pitch velocity, respectively
D	Tube diameter
λ	Complex eigenvalue
μ	The parameter of the constant time delay quasi-steady model
τ	Dimensionless time
$\Phi(\tau)$	Memory function
α_i,δ_i	Memory function parameters
$H(\tau)$	Heaviside step function
$C_D,C_L,\partial C_L/\partial\bar{y}$	Steady drag and lift coefficients, derivative of the lift coefficient with respect to the dimensionless displacement in the lift direction, respectively
k	Reduced frequency
$C(k)$	Equivalent Theodorsen Function
$F(k),G(k)$	The real part and imaginary part of $C(k)$, respectively
$A(k),\phi(k)$	The magnitude and phase of $C(k)$
C_f,ϕ_f	The magnitude and phase of the unsteady fluid force coefficient
C_{da},C_s	Damping and stiffness coefficient, respectively
H_{Fy}	Transfer function between the unsteady fluid force and tube motion

CHAPTER 1 INTRODUCTION

1.1 Research background

Nuclear power as a sustainable energy source plays an important role in society. In 2013, there were 437 nuclear power reactors operated in 31 countries and provided 10% of the world's electricity (IAEA, 2013). In nuclear power plants, steam generators, whose function is to facilitate the heat exchange between two fluid media, have significant effects on the generating efficiency. At first, thermal-hydraulic and heat transfer issues were the primary considerations to enhance the efficiency. Lighter and more slender structures were thus applied. Despite great progress in the improvement of energy output, the specific problem, namely, flow induced vibration (FIV), occurred and became a great concern in the nuclear industry for several decades. It is well known that heat transfer benefits from cross-flow, but higher vibration levels and the possibility of flow-induced instabilities arise. Many incidents of failure in commercial steam generators due to the undesirable vibrations with large amplitudes have been reported (Pettigrew & Taylor, 1991). Almost all heat exchangers, not only limited to steam generators, suffered from this problem during their operation.

Flow-induced vibration (FIV), as the name suggests, is the interaction between fluids and structures that causes excessive vibration. The phenomenon has been studied since 1970s and due to great research effort dedicated to this issue, its mechanism is now better understood. It is generally agreed that four different vibration excitation mechanisms are important in heat exchanger tube arrays. These mechanisms include periodic vortex shedding, random excitation caused by flow turbulence, fluidelastic instability and acoustic resonance (Pettigrew & Taylor, 2003a). The first two kinds of excitation mechanisms are already well known. Periodic vortex shedding takes place when the fluid flow passes over a cylinder at certain velocity. Once the shedding frequency coincides with the natural frequency of the cylinder, excessive vibration will occur and thereby destroy the structure. However, it seems unlikely to happen inside the tube bundles due to the complex structure and high Reynolds number. Pettigrew et al. (2004) carried out detailed flow measurements in a rotated triangular tube array subjected to two-phase cross-flow and identified that even at high void fraction up to 90% no evidence of periodic vortex shedding can be found. The turbulent nature of flow introduces the random pressure fluctuations acting on the surface of

the cylinder which may cause the vibration. Khalvatti (2007) pointed out that turbulence-induced vibrations have little effect on short term damage of the structure but play an important role in the long term wear due to the friction between the tubes and supports. Acoustic resonance occurs in gas flow when the acoustic mode in the tube array matches the vortex shedding frequency. It may amplify the vibration response and create considerable noise leading to fatigue damage.

Fluidelastic instability (FEI) is different in nature from the other types of excitation mechanisms because the fluidelastic forces are motion dependent. The instability depends not only on the flow velocity, but on the tube frequency, the tube bundle configuration and the support effectiveness. This kind of instability has the greatest potential for short term damage to heat exchangers and thus must be avoided in all cases. Figure 1-1 illustrates the amplitude response of a flexible tube in a tube array subjected to cross flow.

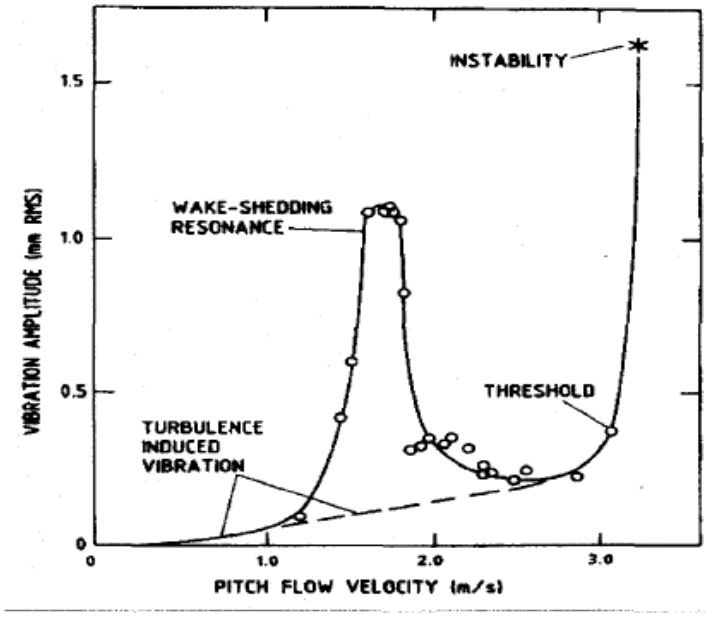

Figure 1-1 : Vibration amplitude of a flexible tube versus pitch flow rate (Pettigrew & Taylor, 1991)

Several theoretical or semi-empirical models have been developed to predict the critical velocity for fluidelastic instability. These include the quasi-static (Blevins, 1974; Connors, 1970), quasi-steady (Price & Paidoussis, 1984), quasi-unsteady models (Granger & Paidoussis, 1996; Meskell,

2009), the analytical channel flow model (Lever & Weaver, 1982) and the unsteady model (Chen, 1987; Tanaka & Takahara, 1981).

The differences among these models lie in the definitions of the dynamic fluidelastic forces. For example, the quasi-steady model was developed based on the position dependent steady fluid forces measured on the tubes. In the analytical channel flow model, the fluid forces are estimated directly using the unsteady Bernoulli equation. The unsteady model was developed by measuring directly the unsteady forces acting on the vibrating tubes. Those models will be reviewed in details in the following chapter.

One of the most important parameters among these models is the time delay, or phase lag, between the tube motion and the fluid forces generated thereby. The quasi-steady model introduced a constant time delay due to retardation of the flow approaching the cylinder (the flow velocity slows down as it nears the cylinder). The quasi-unsteady model proposed a memory effect not the constant time delay and attributed this effect to the reorganization of the viscous wake flow. While in the semi analytical model, this time delay is associated with a mass flow redistribution due to fluid inertia.

The idea of introducing a time delay is not only limit to fluidelastic instability in tube arrays, but also considered in the analysis of flutter of airfoils in unsteady aerodynamics theory. The Wagner's indicial function (Wagner, 1925) and the Theodorsen function (Theodorsen, 1934), which have been widely used for many years, described the time delay between the fluid forces acting on the airfoil and the step transient in the angle of attack in the time domain and the frequency domain, respectively. By reformulating and adapting the expressions of the time delay functions, The Wagner's indicial function and Theodorsen function can also be extended to bluff bodies such as bridge decks (R. H. Scanlan, 1996), square-section cylinders (Luo & Bearman, 1990). Significant successes have been achieved in this extension of unsteady aerodynamics theory. It is, therefore, reasonable to expect that the unsteady aerodynamics theory should be applicable to cylinders in tube arrays to investigate the time delay.

1.2 General objectives and specific objectives

The need to introduce a time delay effect in the fluidelastic instability models is well agreed upon, although the phenomenon behind this time delay is still subject to many possible explanations and

the physics are not well understood. Therefore, the general objective of the research is to investigate the time delay effect for the fluidelastic instability models in order to shed light on the physics of fluidelastic instability. More specifically:

1. The time delay, which specifies the characteristics between the perturbations in the flow and their effects on the tubes, greatly affects the theoretical models. The underlying physics is not fully understood. It is therefore proposed in this work to extend the unsteady aerodynamics theory to the fluidelastic instability model in tube arrays in order to shed more light on the physics of fluidelastic instability.
2. To apply the concept of an Equivalent Theodorsen Function to obtain the time delay formulation for tube arrays in a frequency domain representation.
3. To measure the unsteady fluid forces and quasi-static forces in a rotated triangular tube array subjected to water flow for determining the Equivalent Theodorsen Function.
4. To conduct the stability analysis of predicting the critical velocity for fluidelastic instability and to evaluate the performance of the newly proposed model

1.3 Methodologies

It is well known that FEI may occur even for a single flexible cylinder in a rigid tube array subjected to cross flow. Lever and Weaver (1986) pointed out that the single flexible tube in the rotated triangular tube array has essentially the same critical velocity as the corresponding fully flexible tube array and the dynamic instability occurs in the transverse direction. For simplicity, consideration is given here to the particular case of a single flexible tube in an otherwise rigid tube array which is free to move in the transverse direction. We note, however, that the time delay function to be developed remains valid for fully flexible arrays with appropriate considerations.

The determination of the time delay formulation will be done by measuring the unsteady and quasi-static fluid force coefficients in a rotated triangular tube array subject to water flow with a pitch ratio of 1.5. The unsteady fluid forces can be measured by integration of the pressure field on the surface of the tubes, or be measured indirectly by using the force sensor instrumented on the tube. In the latter case, the inertia of the tube and the fluid added mass are, however, incorporated in the measured forces. The added mass is measured in still water and a relatively high frequencies. A

transfer function between the fluid force and the displacement of the vibrating tube can be applied to obtain the fluid force coefficients from the measured forces.

To validate the theoretical model, stability analysis will be conducted and compared with experiments. Considering the limitation of time, the experimental stability test will not be conducted in the present work. Instead, the experimental results from the literature (Sawadogo & Mureithi, 2014b; Violette et al., 2006; D. t. Weaver & Fitzpatrick, 1988) will be used for comparison.

1.4 Presentation of the thesis

The main work done to develop a time delay formulation for FEI model is presented in Chapter 3 as a journal article. Firstly, a time delay formulation using the concept of the Equivalent Theodorsen Function was developed in the frequency domain. A test section was designed to measure the unsteady and static fluid forces. The test section includes a rotated triangular tube array with a pitch ratio of 1.5, a linear motor which is mounted on the central tube, instrumented with a force sensor ATI Nano25 and a displacement system allowing the tube to be displaced in the transverse direction. The Equivalent Theodorsen Function which is developed in a frequency domain representation was extracted from the experimental data. It was compared with the other time delay functions. Using the Equivalent Theodorsen Function, a stability analysis was conducted to predict the critical velocity for fluidelastic instability. The theoretical results were compared with experimental data and other FEI models to assess the validity of the proposed model.

The Reynolds number effect on the force coefficients on the central tube in a rotated triangular tube array is investigated based on CFD in Chapter 4. Some results presented in Chapter 3 are discussed in Chapter 5. Some supplementary discussions are also presented in Chapter 5, including the flow periodicities in tube arrays, the general relation of time delay function for aeroelastic systems and the limitation of the stability analysis. Conclusions and recommendations for future work are presented in Chapter 6.

CHAPTER 2 LITERATURE REVIEW

2.1 The nature of fluidelastic instability in tube arrays

Fluidelastic instability is a self-excitation mechanism due to the motion-dependent forces. In tube arrays, when a tube is subjected to cross flow, the tube moves from its initial (equilibrium) position. The displacement causes a further change in the fluid force acting on the tube. The damping force absorbs the energy to back its equilibrium position to compete with the fluid force. From the viewpoint of energy, if the energy consumed by damping force exceeds the energy input by the fluid force, the vibrations die out. Conversely, if enough energy is provided to sustain the vibration, the amplitude will grow rapidly. This occurs when the flow velocity exceeds a critical threshold level which is called the critical velocity. Once instability occurs the tube will be damaged by fretting wear at the supports, by clashing with neighbouring tubes or by fatigue.

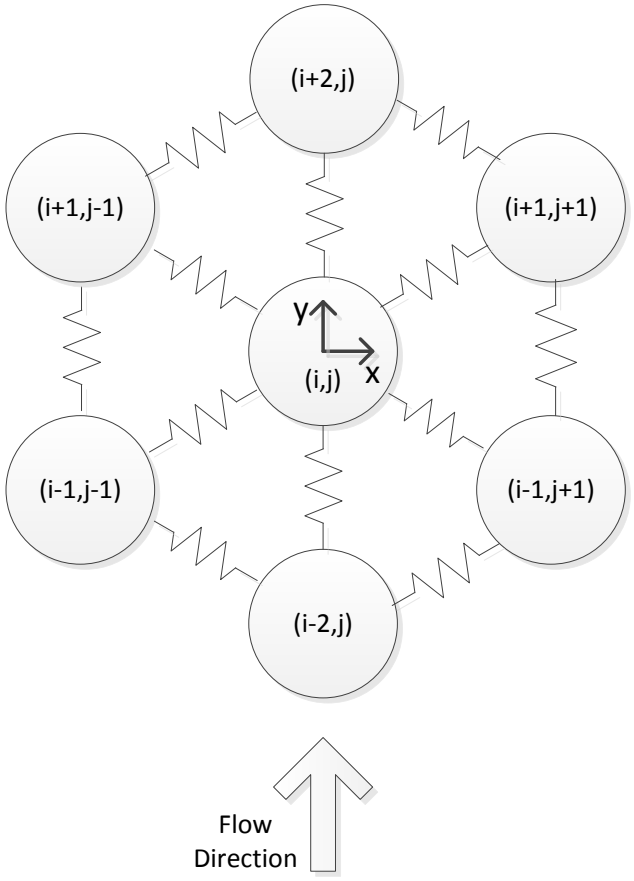

Figure 2-1 : A tube array subjected to cross-flow

To describe the fluidelastic instability in a tube array subjected to cross-flow as shown in Figure 2-1 in detail, the general equation of motion for the system can be written as (Chen, 1987)

$$[M]\{\ddot{X}\}+[C]\{\dot{X}\}+[K]\{X\}=F_e \tag{2.1}$$

or

$$[M_s+M_f]\{\ddot{X}\}+[C_s-C_f]\{\dot{X}\}+[K_s-K_f]\{X\}=F_e \tag{2.2}$$

where $[M],[C],[K]$ are the mass, damping and stiffness matrixes, respectively. The subscripts s and f represent structure and fluid, respectively. $\{\ddot{X}\}$ represents the tube acceleration vector, $\{\dot{X}\}$ the tubes velocity vector and $\{X\}$ the tubes displacement vector. F_e is the external forcing term. It should be noted that $[M],[C],[K]$ are functions of $\{\ddot{X}\},\{\dot{X}\},\{X\}$ in general.

From the viewpoint of dynamics, the system is considered to be stable if both modal damping and stiffness terms are positive. The modal stiffness terms switch from positive to negative indicates the occurrence of static instability, also known as divergence. Dynamic instability occurs when physically there is a net energy increase per oscillation causing a dramatic growth in response amplitude as shown in Figure 1-1. It may be caused by two distinct mechanisms: damping (or velocity) controlled and stiffness (or displacement) controlled instability (Chen, 1987).

Damping controlled instability take place when the net damping switches from positive to negative. It only needs one degree-of-freedom (Lift direction). The fluid force producing instability is in phase with the tube velocity. Stiffness controlled instability is caused by the antisymmetric stiffness term. It is also called coupled mode flutter (in aeroelasticity) since at least two modes are required such that the relative motion between tubes can produce the force to overcome the structural damping. In this kind of instability the fluid forces are in phase with the tube displacements.

Some theoretical or semi-empirical FEI models have been developed to predict the critical velocity such as the quasi-static (Blevins, 1974; Connors, 1970), the quasi-steady (Price & Paidoussis, 1984), the quasi-unsteady model (Granger & Paidoussis, 1996; Meskell, 2009), the semi-analytical channel flow model (Lever & Weaver, 1982) and the unsteady model (Chen, 1987; Tanaka & Takahara, 1981). The differences among these models lie in the definitions of the dynamic fluidelastic forces. For example, the quasi-steady model was developed based on the steady fluid forces measured on the tube placed at various positions. In the channel flow model, the fluid forces

are estimated directly using the unsteady Bernoulli equation. The unsteady model was developed by measuring directly the unsteady forces acting on the vibrating tubes. One of the most important parameters among these models is the time delay, or phase lag, between the tube motion and the fluid forces generated thereby. In general, for a cylinder subjected to a cross-flow, the flow-induced forces acting on it will be time dependent as a consequence of motion or turbulence in the approaching flow. When a sudden change happens in the position of the cylinder relative to the cross-flow, a transient is initiated in the associated force acting on the cylinder. This is typically not instantaneous but takes some time to develop. This time taken to develop the steady fluid force is the time delay. The main goal of the present work is to develop a new time delay formulation for FEI models and to shed light on the physics of FEI. First, a brief review of some fundamental FEI models is presented as follows

2.2 Theoretical models for fluidelastic instability

2.2.1 Jet-Switching model

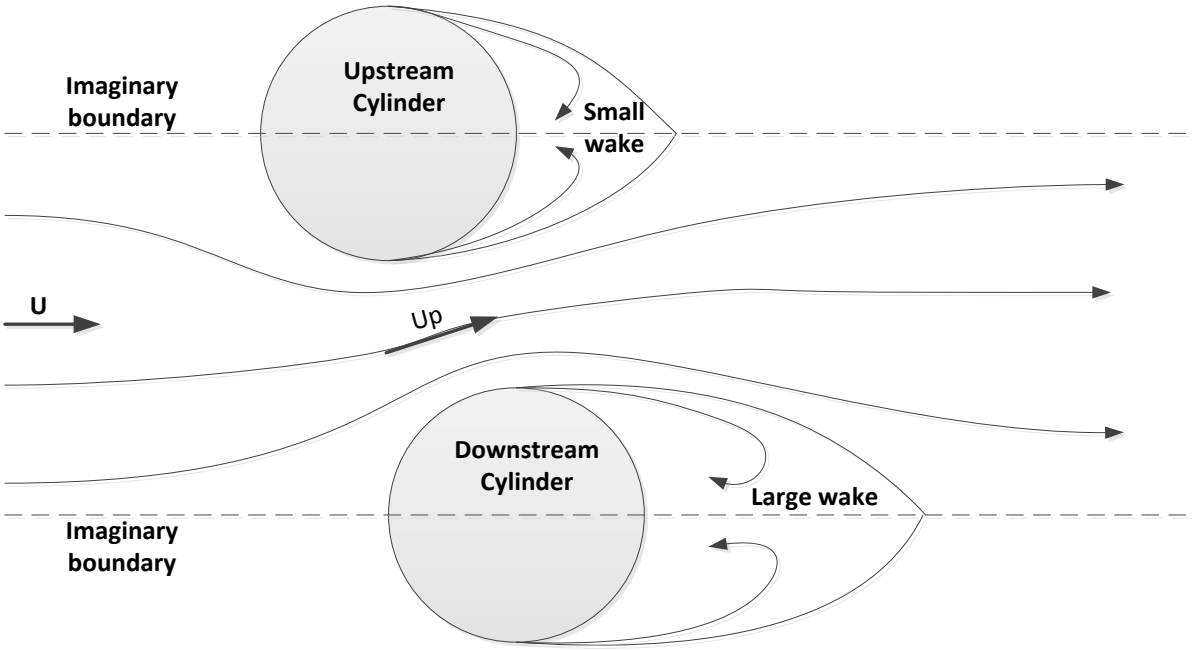

Figure 2-2 : Jet-Switching model

The Jet-Switch model, proposed by Roberts, is the first semi-analytical model to study fluidelastic instability in tube arrays subjected to cross flow. Roberts found that the fluid jets developed behind a single row of cylinders subjected to cross flow. The instability was limited to the in-flow direction building on his preliminary experiments. A hypothetical channel flow was proposed as shown in Figure 2-2. The flow through two rows of cylinders is represented by two wake regions (one large and one small) developed behind the two adjacent downstream half cylinders, a jet flow between them and imaginary boundaries. The jet switched as the cylinder was moving upstream and downstream, inducing a variation in the pressure distribution and thus a variation of drag force, resulting in fluidelastic instability. Assuming that the flow separation occurs at the minimum cross section between the cylinders, that the flow upstream of separation points and in the jet region is inviscid, and the pressure in the wake regions to be constant, the pressure distribution can be obtained analytically and then the drag force can be achieved by integration. He obtained equation (2.3) for the critical velocity by neglecting both the effects of unsteady and fluid damping.

$$\frac{U_c}{\omega_n \varepsilon D} = K\left(\frac{m\delta}{\rho D^2}\right)^{0.5} \tag{2.3}$$

where ε is the ratio of fluidelastic frequency to structural frequency, which is approximately 1. U_c is the critical flow velocity, f is the tube natural frequency, $m/\rho D^2$ is the non-dimensional mass parameter, δ is the logarithmic decrement and K is the constant. It is the initial form of the well-known Connors equation.

Although the jet-switch model showed a poor agreement with experiments because of the fact that most experiments indicated that instability predominantly occur normal to flow, the analysis shed some light on the mechanism of fluidelastic instability, including the consideration of the time delay effect and the initial form of Connors equation.

2.2.2 Quasi-Static model

The quasi-static model can be understood through the idea that the motion of the tube is sufficiently slow such that the fluid-dynamic forces acting on the cylinder oscillating in flow are equal to, at any instant of time, the forces on the stationary cylinders in the identical position. The quasi-static model was first developed by Connors for the instability of a single row of cylinders subjected to cross flow. The author observed that the main oscillating patterns of the cylinders when instability

occurs are elliptical orbits either streamwise or in the cross-stream direction. Given the fact that jet switching cannot occur for low U/fD, he concluded that jet switching is not the mechanism leading to instability. Connors measured the fluid force coefficients instead of determining them analytically. By neglecting the fluid damping terms and performing an energy balances in the in-flow and cross-flow directions, Connors obtained the most famous expression for fluidelastic instability as follows:

$$\frac{U_c}{fD} = K\left(\frac{m\delta}{\rho D^2}\right)^{0.5} \tag{2.4}$$

where K is the Connors constant for which Connors obtained as 9.9 for the tube row.

Connors model achieved reasonable success in the engineering field due to its simplicity and satisfactory accuracy. It was used to design tube bundles of various geometrical arrangements by choosing the appropriate value of K. Blevins (1974) also formalized this expression mathematically and extended the quasi-static model to analyze tube arrays. He suggested that the constant K needs to be changed depending on the tube array. H. Connors (1978) also demonstrated that the constant is a function of the tube pattern and spacing. He obtained the correlation $K = \left[0.37 + 1.76\left(T/D\right)\right]$ for $1.41 \le T/D \le 2.12$ based on experimental results, where T is the separation between cylinders in a row. Pettigrew (1978) extended the quasi-static model to the two-phase flow and suggested a conservative value of $K = 3.0$ based on a number of experimental observations.

However, the quasi-static theory does not always hold well when compared with experimental results. The quasi static theory is limited, as Tanaka and Takahara (1981) pointed out, since the quasi-static fluid force is always in phase with the displacement (only dependent on displacement) and the effect of the unsteady fluid force component is ignored.

2.2.3 Unsteady model

Tanaka and Takahara (1980, 1981) presented an unsteady model which takes into consideration all components of the fluid dynamic forces. The square tube array with 4 rows and 7 columns and the pitch ratio of 1.33 was considered as shown in Figure 2-3. The fluid force acting on the cylinder C

was assumed to be induced by the cylinder itself and the four neighbouring cylinders numbered as 1-4. The unsteady drag and lift forces acting on the cylinder were then expressed as

$$\begin{aligned} F_x &= \frac{1}{2}\rho U^2\left[C_{xcx}x_c + C_{x2x}\left(x_2 + x_4\right) + C_{x2y}(y_2 - y_4) + C_{x1x}x_1 + C_{x3x}x_3\right] \\ F_y &= \frac{1}{2}\rho U^2\left[C_{ycy}y_c + C_{y2y}\left(y_2 - y_4\right) + C_{y2y}(y_2 + y_4) + C_{y1y}y_1 + C_{y3y}y_3\right] \end{aligned} \tag{2.5}$$

where C_{xcx}, C_{ycy}, etc. are the fluid dynamic force coefficients, in which the first subscript gives the force direction, the second gives the position of the vibrating cylinder and the last subscript is the vibrating direction of the cylinder, respectively. The unsteady fluid forces acting on the cylinder were therefore measured by vibrating these five cylinders separately to obtain the corresponding force coefficients.

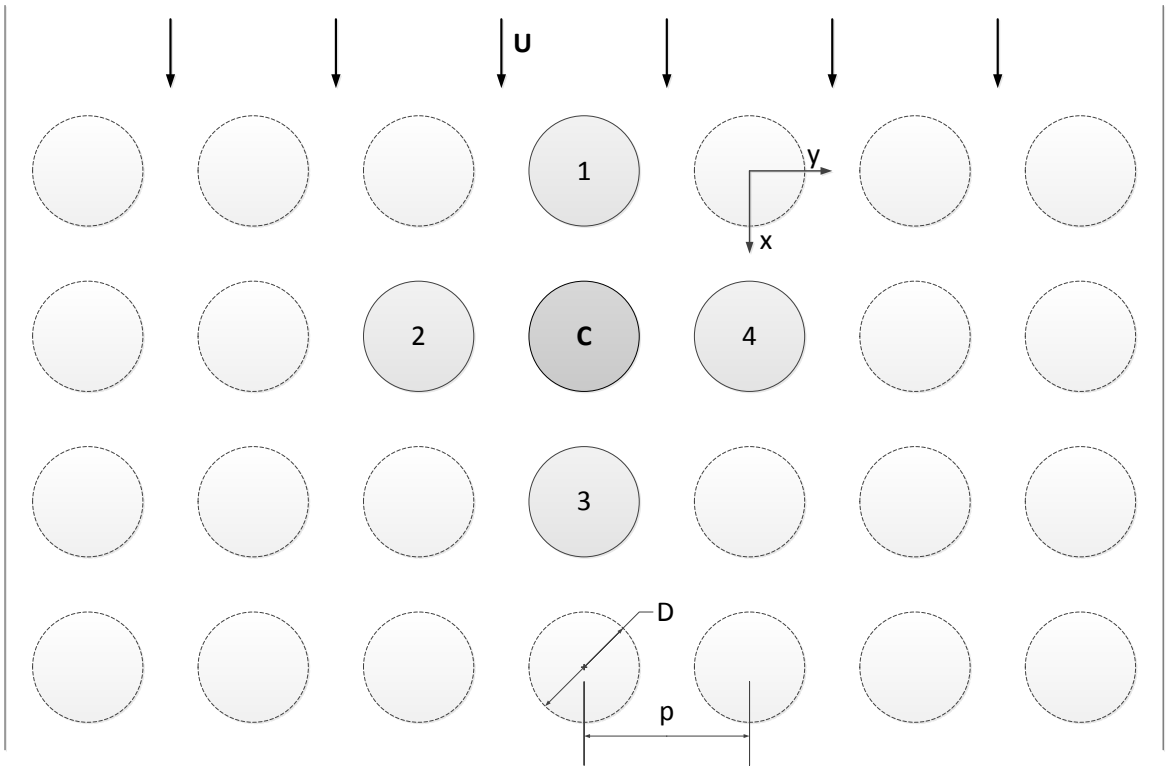

Figure 2-3 : Unsteady model

The critical velocity in air and water flow was then investigated using their measured unsteady force coefficients. The results showed that calculated critical velocities in water flow are a little less than the experiment data, while it is in quite good agreement with experiment data for air flow.

Tanaka and Takahara studied the effect of fluid density on critical velocity and gave the expressions for critical velocity as follows:

$$\begin{aligned} \frac{U_c}{fd} &= K\left[\frac{m\delta}{\rho d^2}\right]^{0.5}\delta^{0.5} \qquad \text{for low density fluid} \\ \frac{U_c}{fd} &= K\left[\frac{m}{\rho d^2}\right]^{1/3}\delta^{1/5} \qquad \text{for high density fluid} \end{aligned} \tag{2.6}$$

They also investigated the effect of detuning of the natural frequency on the critical velocity by varying the frequency of test tubes slightly. The critical velocity increases with detuning indicating that detuning of the natural frequency has a stabilizing effect.

Chen (1987) developed an analytical expression for the fluid forces based on the unsteady flow theory. His work proved that the other theories, such as quasi-static, quasi-steady, quasi-unsteady models, are special forms of the unsteady flow theory depending on the assumptions. The coefficients in the analytical expression were calculated by Chen and Jendrzejczyk (1983) based on Tanaka and Takahara's data (1980, 1981; 1982). The authors proposed that the dynamic instability can be classified into two mechanisms: fluid-damping-controlled and fluid stiffness-controlled instabilities.

Although the unsteady model gives excellent agreement with experimental results, a great experimental effort is required to obtain the unsteady fluid force coefficients. As a practical tool of tube array design, the unsteady model is not considered to be the idea option.

2.2.4 Semi-analytical model

Based on experiments showing that a single flexible cylinder in a rigid array could have essentially the same critical velocity as the fully flexible tube array, Lever and Weaver (1982) developed the first semi-analytical model based on a single flexible tube in a unit cell of rigid tubes subjected to cross-flow as shown in Figure 2-4. The flow pattern is divided into two regions, streamtube or channel regions and front stagnation and wake regions. The key assumption of the model is that the excitation mechanism derives from motion dependent fluid forces in the streamtube regions. The flow near the front stagnation point and in the wake behind the cylinder was not considered as they argued that the flow in these regions has little effect on the stability in the transverse direction. The time delay was proposed as follows

$$\tau = l / U_0 \tag{2.7}$$

where l is the length of the streamtube and U_0 the upstream velocity. The authors assumed that the time delay originates from the mass flow redistribution lagging behind the tube variation due to the finite fluid inertia. The pressure distribution around the cylinder was solved analytically by applying the unsteady Bernoulli equation and as a result the fluid forces could be calculated.

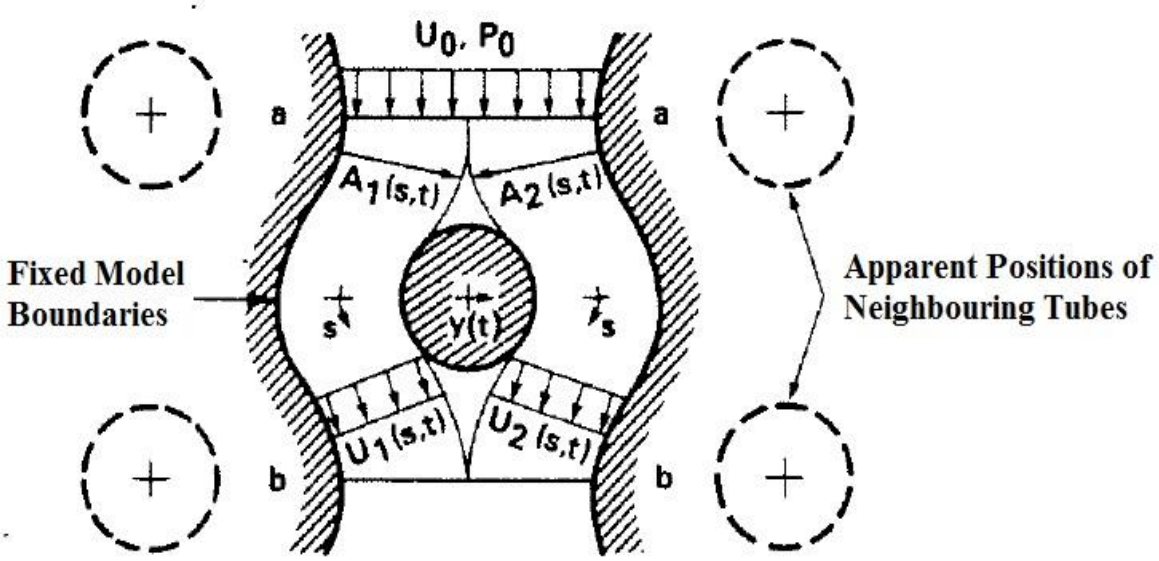

Figure 2-4 : Semi-analytical model (Lever & Weaver, 1982)

Lever and Weaver (1986) modified the analytical model to describe the static and dynamic instability in the transverse and streamwise directions. The authors suggested that there is no flow redistribution in streamwise direction and thereby no dynamic instability in streamwise direction is predicted by the model. However, static instability was found to exist in both transverse and streamwise directions.

Yetisir and Weaver (1993) refined the theoretical model by introducing some assumptions, such as the disturbance decay function which accounts for flow perturbation due to the tube motion, phase function as well as flow attachment and separation points. The authors also extended the model to multiple flexible tubes in the array. The results indicated that the damping mechanism is predominant at low mass damping parameter, and the stiffness mechanism is predominant at high mass damping parameters with regard to fluidelastic instability. This finding is in considerable agreement with the quasi-steady model (Price & Paidoussis, 1984).

2.2.5 Quasi-Steady model

Price and Paidoussis (1984) developed the quasi-steady model for the fluidelastic instability of a double row of flexible tubes subjected to cross-flow as shown in Figure 2-5. The author assumed that the fluid forces acting on a tube are affected only by two adjacent tubes and the tube itself. The tube movement changes the resultant flow velocity of the fluid, the drag and lift forces are then parallel and normal to the resultant velocity, respectively. The coefficients of fluid forces were developed in a Taylor expansion using the coordinates of the surrounding cylinders.

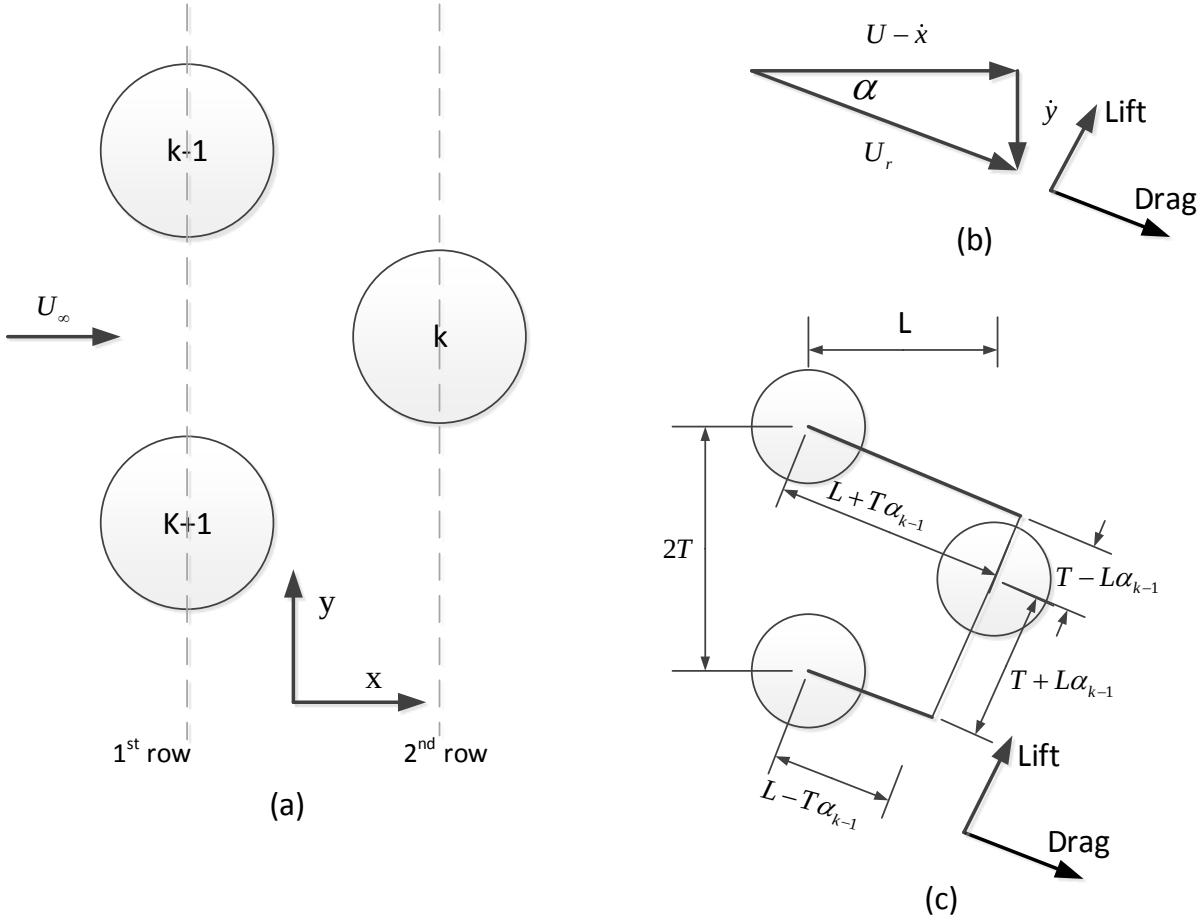

Figure 2-5 : Quasi-Steady model

The fluid dynamics of a typical downstream cylinder k (see Figure 2-5 (a)) are considered. U_∞ is the free-stream flow velocity. The inclination angle of the relative flow velocity is donated by α as shown in Figure 2-5(b). The forces on cylinder k depend on the motion of cylinder $k+1$ and $k-1$ as well as on its own motion. It is, therefore, necessary to determine the apparent displacement of cylinder $k+1$ and $k-1$ as seen from cylinder k (see Figure 2-5 (c)).

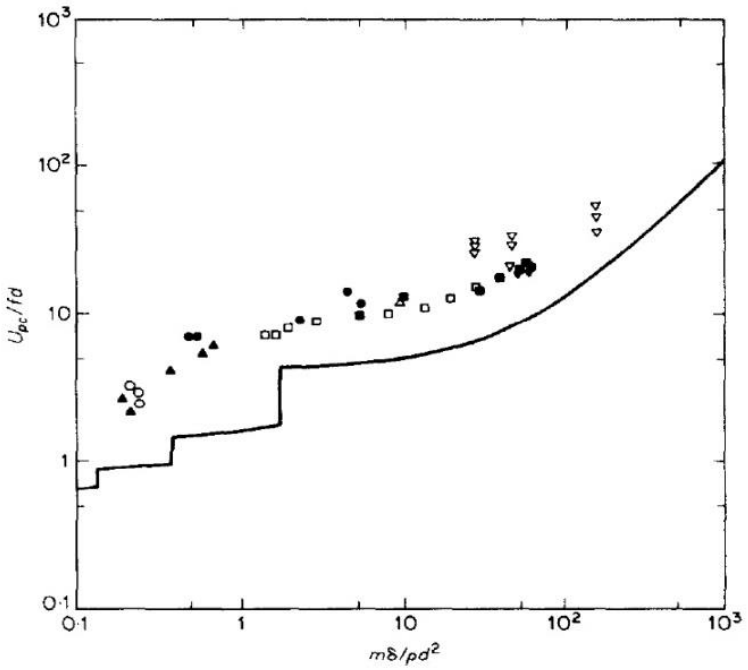

Figure 2-6 : A comparison between the theoretical stability threshold and the experimental data for a single flexible cylinder in an array of rigid cylinders (Price & Paidoussis, 1984). Experimental data: Δ, Connors (1980); O, Gorman (1976); ∇, Hartlen (1974); ▲, Heilker and Vincent (1981); ●, Pettigrew *et al.* (1978); ▼, Soper (1980); □, Weaver and Grover (1978); ■, Weaver and El-Kashlan (1981).

A time delay of the fluid forces relative to the movement of the tubes was proposed. This effect was incorporated in the model, resulting in frequency-dependent terms contained in the stiffness and damping matrices. It is worth noting that the time delay arises from two aspects: (i) the time taken for the flow leaving an upstream cylinder to arrive at a downstream cylinder; (ii) the retardation of the flow approaching the cylinders. Using potential flow theory, the time delay due to flow retardation is expressed as follows:

$$\tau = \mu \frac{D}{U_p} \tag{2.8}$$

where U_P is the fluid velocity, D the tube diameter, and μ the time delay coefficient which is taken to be of order 1 as suggested by Simpson and Flower (1977). As the time delay coefficient is always taken as a constant, the quasi-steady model is also called the constant time delay model.

The comparison between the theoretical prediction of this model and the experimental stability boundaries for a single flexible cylinder in an array of rigid cylinders is shown in Figure 2-6. Although the quantitative agreement is not satisfactory, the slopes of the theoretical curve and experimental data are similar.

The authors pointed out that the fluidelastic instability is governed by the (i) negative fluid damping mechanism for $m\delta/\rho d^2 < 300$ and (ii) stiffness controlled mechanism for $m\delta/\rho d^2 > 300$. Moreover, the authors suggested that the mass term and damping term in the Connors-type expression should not be lumped together for stiffness-controlled instability.

Price and Paidoussis (1986) extended this model to analyze the fluidelastic instability for a single flexible cylinder in an otherwise rigid array. The time delay parameter is taken to be unity, which appears to give the best agreement between theory and experiments. An improved prediction is obtained in an in-line square array with P/D=1.5. The authors also confirmed Lever and Weaver's observation (Lever & Weaver, 1982) that for $m\delta/\rho d^2 < 300$, the single flexible cylinder in the midst of an array of rigid cylinders has approximately the same stability boundary as fully flexible array.

2.2.6 Quasi-Unsteady model

Granger and Paidoussis (1996) proposed an improvement to the quasi-steady model, namely the quasi-unsteady model, where the most important unsteady effects are considered. The continuity and Navier-Stokes equations were applied to develop the fluid forces induced by an impulsive motion of a body subject to cross-flow. A memory effect, rather than a constant time delay, was established. The authors postulated that the memory effect is due to the diffusion-convection process of the vorticity induced by the motion of the cylinder. The physics of time delay may be described as follows: a perturbation of the tube velocity disturbs the flow field in the neighborhood of the tube. The perturbation in the fluid force acting on the tube is therefore induced and decays continuously with time as the vorticity is transported downstream. The new steady state is obtained after the vorticity has been conveyed far away from the tube by the mean flow.

The modified fluid force is expressed as follows:

$$F_f = -\left[M_f\right]\{\ddot{x}\} + \left[C_f\right]\{\dot{x}\} + \left[K_f\right]\{h * x\} \tag{2.9}$$

where $[M_f],[C_f],[K_f]$ are the added mass, damping and stiffness matrices of the fluid. The convolution function which is in terms of the dimensionless time$\tau(\tau = Ut/D)$ in Eqn. (2.9) is defined as follows:

$$h * x = \int_0^{\tau} \frac{d\Phi(\tau - \tau_0)}{d\tau} x(\tau_0)\, d\tau_0 \tag{2.10}$$

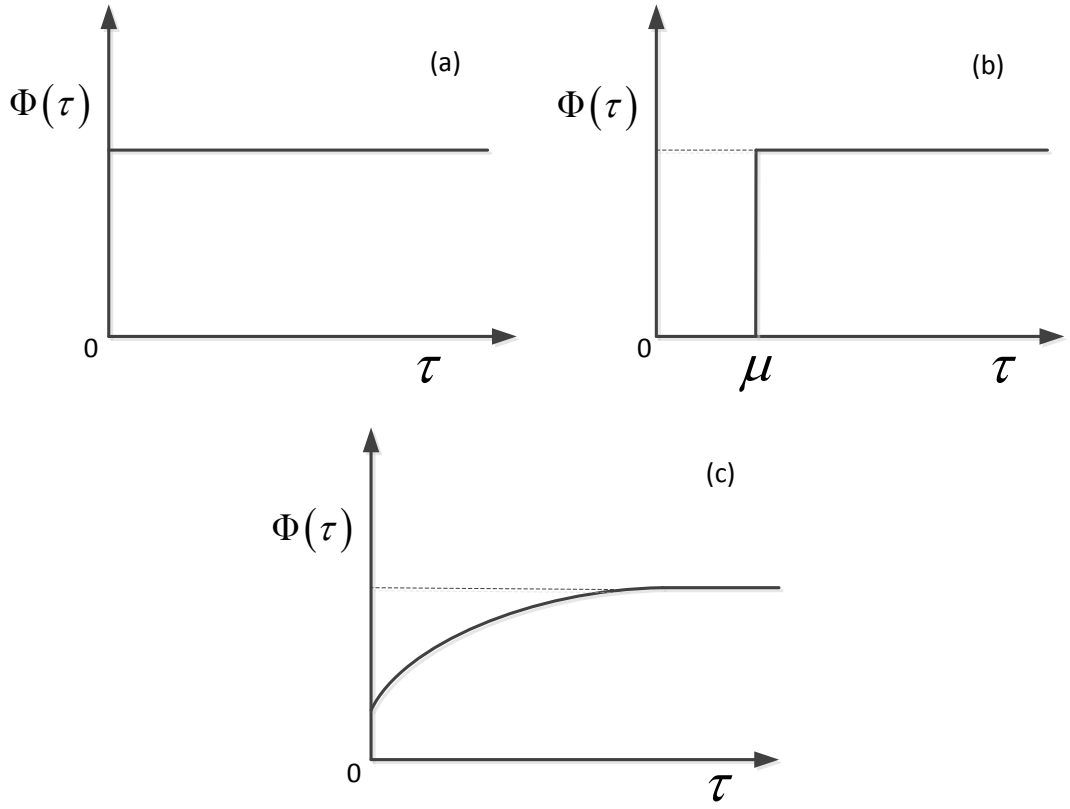

Figure 2-7 : Comparison of different time delay models. (a) quasi-static model; (b) quasi-steady model; (c) quasi-unsteady model.

In Eqn. (2.10), $\Phi(\tau)$ is the time delay function, or memory function, which is of key interest to the quasi-unsteady model. The memory function, which accounts for the time delay, tends to one as $\tau \to +\infty$. This can be approximated by a linear combination of decaying exponentials and a Heaviside step function $H(\tau)$ as follows

$$\Phi(\tau) = \left[1 - \sum_{i=1}^{N} \alpha_i e^{-\delta_i \tau}\right] H(\tau) \tag{2.11}$$

It is noteworthy that this memory function forms a general framework for the foregoing models. The quasi-static model can be retrieved by setting $\alpha_i = \delta_i = 0$, and the quasi-steady model by setting $\alpha_i = \delta_i = 0, H(\tau) = H(\tau - \mu)$. The values for α_i and δ_i in this model were obtained with experimental data.

The different transient behaviors of the lift coefficient for the quasi-steady and quasi-unsteady models are shown in Figure 2-7.

To support the assumption of the physics of the time delay proposed by Granger and Paidoussis (1996), Meskell (2009) proposed a simple wake model to clarify that the underlying process of vorticity transport accounts for the time delay. The memory function is obtained by numerical integration of the governing equations without calibrating the model with experimental data.

Although the memory effect may appear novel in a quasi-unsteady analysis, the use of memory effect is far from new, and as early as 1950, this effect was deemed to be important in the unsteady airfoil theory. It is worth noting that if the transient function of the quasi-unsteady model is taken as the Wagner's function (Wagner, 1925), the lift force acting on the cylinder is the same as the lift force acting on the airfoil due to the growth of circulation. since we believe that the unsteady airfoil theory has a degree of generality and is also applicable to the cylinder, the extension of the theory will be briefly introduced later.

2.2.7 Computational Fluid Dynamics model

To study fluid-structure interaction problems, Computational Fluid Dynamics (CFD) has a great advantage over the other methods at solving the governing equations. The developments in CFD and the availability of more powerful computers have paved the way for the modeling and predicting fluidelastic instability. Due to the high turbulence and viscous effects of the fluid flow inside the tube arrays, the full Navier-Stokes equations with moving boundaries are required to simulate the tube motions. Kassera and Strohmeier (1997) used the $k-\varepsilon$ turbulence model to predict the flow-induced vibrations of six different tube bundles. Although they could not predict the correct critical velocity for fluidelastic instability, the simulations of vibration amplitudes agreed well with experiment data for low Reynolds numbers. Schröder and Gelbe (1999) carried out two- and three-dimensional CFD simulations to predict fluidelastic instability in tube bundles. The $k-\varepsilon$ and $k-\omega$ turbulence models were compared and the simulations indicated that the

$k-\omega$ model provides the best results. However, the predicted critical velocities were too low compared with experimental results. Khalifa et al. (2013) developed a simplified two-dimensional CFD model for a parallel triangular tube array with a pitch ratio of 1.54. The Reynolds Averaged Navier-Stokes equations (RANS) and the Shear Stress Transport (SST) turbulence model were used. The moving boundaries were employed to obtain the flow velocities and time dependent pressure distributions. The surface pressure distributions given by the CFD results were in good qualitative agreement with the experiments of Mahon and Meskell (2012). The phase lag function obtained from the CFD results was then applied in the Lever and Weaver's semi-analytical model for FEI. A significant improvement of the predictions was provided by the model, especially for low reduced velocity which eliminated the infinite stability regions.

Although computational fluid dynamics (CFD) has improved significantly in recent years, no computational model, at least at present, can solve the fully coupled governing equations with the tube motion equations for practical Reynolds numbers and provide reliable predictions for fluidelastic instability.

2.3 Extension of unsteady aerodynamics theory

It is worth noting that the memory function $\Phi(\tau)$ in Eqn.(2.11) is identical to the approximate expression of the Wagner function of unsteady aerodynamics theory. Luo and Bearman (1990) applied the unsteady aerodynamics theory to estimate the fluctuating lift force induced by the transverse oscillation of a square-section cylinder. This model improved agreement between theory and the experiments which shows that the unsteady aerodynamics theory should have a certain degree of generality and may also be applicable to cylinders in tube array.

In unsteady aerodynamics theory, descriptions in both time- and frequency- domains of the aerodynamic forces acting on the thin airfoils have been applied in the aeroelastic analysis models of airfoils with reasonable success. Among the wide range of unsteady aerodynamics models, the classical models of Wagner (1925) and Theodorsen (1934) remain widely used for over three-quarters of a century. These two models will be reviewed briefly as follows and the interested reader is referred to Fung (2002) for more detailed information.

Wagner proposed the so-called indicial function which gives the relationship between the indicial lift force and the transient step change in angle of attack of an airfoil in an inviscid flow. If the

airfoil experiences an abrupt step-function change from steady state to an incremental angle of attack α_0 in an incompressible fluid, the lift force undergoes a transient change expressed as follows:

$$L(\tau) = 2\pi b\rho U^2 \alpha_0 \Phi(\tau) \tag{2.12}$$

where $\tau = Ut/b$ is a non-dimensional time, b the half chord of the airfoil. The function $\Phi(\tau)$, called Wagner's function or the indicial function, is illustrated in Figure 2-8.

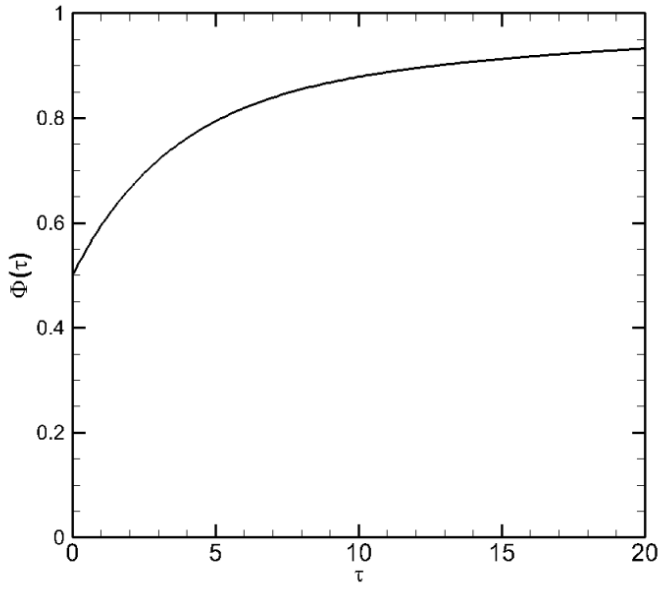

Figure 2-8 : Wagner's function for an incompressible fluid.

Theodorsen obtained a transfer function in terms of the lift force and the motion of the airfoil under harmonic oscillations. Assuming a thin airfoil undergoing harmonic vertical (h) and torsional (α_t) motion in a potential flow:

$$h = h_0 e^{i\omega t} = h_0 e^{ik\tau}, \quad \alpha_t = \alpha_0 e^{i\omega t} = \alpha_0 e^{ik\tau} \tag{2.13}$$

where $k = \omega b/U$ is the reduced frequency

The theoretical lift force can be expressed as follows:

$$L(\tau) = \pi\rho b^2 (U\dot{\alpha}_t + \ddot{h} - ab\ddot{\alpha}_t) + 2\pi b\rho UC(k)\left(U\alpha_t + \dot{h} + b(0.5 - \alpha_t)\dot{\alpha}_t\right) \tag{2.14}$$

where ab is the distance from the airfoil midchord to the oscillatory rotation point and the function $C(k)$ is the renowned Theodorsen function

$$C(k) = F(k) + iG(k) \tag{2.15}$$

originally expressed in terms of Bessel or Hankel functions. The function F and G are plotted in Figure 2-9. It should be noted that although the lift force is expressed in the time domain, the Theodorsen function is defined in the frequency domain which is the built-in characteristic of the classical flutter theory.

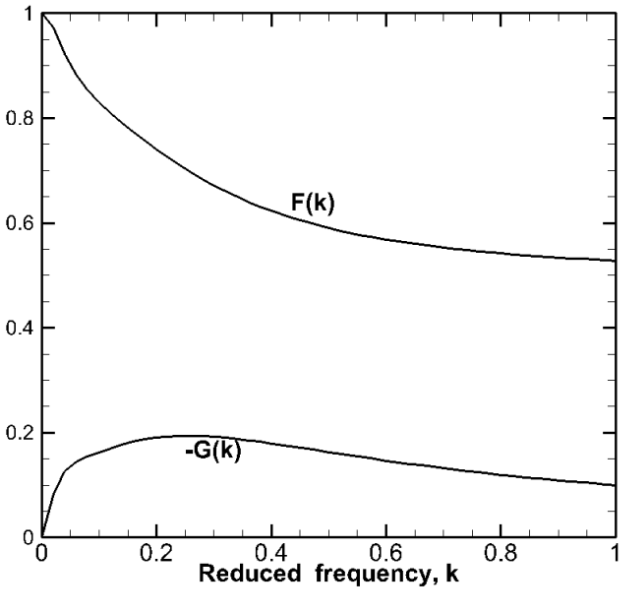

Figure 2-9 : Real and imaginary components of Theodorsen function.

For a harmonic motion consisting only of the vertical velocity $\dot{h}$ the lift force according to Eqn. (2.14) is

$$L(\tau) = 2\pi\rho b U^2 \alpha_t C(k) \tag{2.16}$$

where

$$\alpha_t = \dot{h}/U$$

Garrick (1938) and Jones (1938) observed that Theodorsen and Wagner functions are equivalent representations of the effect of the wake (the lift force due to circulation) in the frequency domain

and time domain, respectively. It is worth noting that the time-domain indicial function developed by Wagner, and the frequency domain formulation proposed by Theodorsen are obtained with the hypothesis of inviscid and fully attached flow.

These descriptions both in time-domain and frequency-domain, were not only employed to the motion-induced forces on the streamlined airfoil, but reorganized and adjusted to the nonstreamlined bodies, such as the bridge decks (R. H. Scanlan, 1996) and rectangular cylinders (Hatanaka & Tanaka, 2008). In these cases, the vortex shedding, flow separation, reattachment and other possible unsteady effects may occur in the flow which is not compatible with the hypothesis mentioned before. The analytical closed-form formulations for the motion-induced forces are hence not available. Nevertheless, several approaches have been developed to overcome such a drawback.

In the cases of frequency-domain approaches, it is common practice to obtain the frequency-dependent functions (namely, the flutter derivatives or aeroelastic derivatives which are similar to the Theodorsen function) by experimental means (Miranda，S, 2013). In the context of bridge decks, the aerodynamic loads acting on bridge sections were expressed in a linearized format. The flutter derivatives were evaluated by forcing a harmonic motion on the section and extracting the derivatives via the method of least squares (Simiu & Scanlan, 1996).

As regards the time-domain approaches, great challenges exist in the experimental evaluation of the indicial function (similar to the Wagner function) due to the difficulties arising in the direct measurements of the response to step motions. The computational fluid dynamics (CFD) approaches have therefore been developed to obtain the indicial function, such as in the work of Farsani et al. (2014), Hatanaka and Tanaka (2008) and Braun and Awruch (2003). R. Scanlan (2000) first presented the interrelationships between the indicial functions and the flutter derivatives. An indicial function for the bluff section was achieved based upon the measured flutter derivatives.

2.4 Summary

In the previous sections, the different vibration mechanisms including periodic vortex shedding or more generally, flow periodicities, random excitation caused by turbulent flow, fluidelastic instability and acoustic resonance have been described. It is generally agreed that fluidelastic

instability is the most severe case which has the great potential for short term damage to heat exchangers.

Several theoretical models for fluidelastic instability were also presented. The jet-switching model confined the instability in the in-flow direction which is not in accord with most experiments which indicate that instability predominantly occurs in the direction transverse to the flow. Connor's model is the most popular model in industry because of its simplicity and satisfied accuracy. However, the phase between the fluid force and the displacement and the effect of unsteady fluid force are ignored. Besides, the Connors model can only predict the critical velocity. Therefore, interest in the study of the vibration response of the structure before and after the instability cannot be answered. The unsteady model gives the best agreement with experimental results. Nevertheless, it requires a great effort in the unsteady fluid force measurements which indicates that it is not the priority as a practical model for the tube array design. In the semi-analytical model, the fluid forces are obtained using unsteady Bernoulli equation. The model can only predict the instability in cross-flow direction and fails to predict the stiffness-controlled instability. Recently, Hassan and Weaver (2016) attempted to extend this model to predict streamwise instability. The quasi-steady and quasi-unsteady models, on the other hand, have the advantage of requiring less experiment effort and overcome the theoretical problems mentioned above. The main difference between the quasi-steady and quasi-unsteady models is the definition of the induced time delay.

As previously noted, from the very beginning of the jet switch model, quasi-static model to the sophisticated quasi-steady, quasi-unsteady and semi-analytical model and then to the more general unsteady model, one of the most important parameters among these models is the time delay, or phase lag, between the tube motion and the fluid forces generated thereby. In the semi-analytical model, the time delay originates from the mass flow redistribution lagging behind the tube motion due to the finite fluid inertia. A constant time delay was introduced in the quasi-steady model. The origin of time delay arises from two aspects: (i) the time taken for the flow leaving an upstream cylinder and arriving at a downstream cylinder; (ii) the retardation of the flow approaching the cylinders. Later, it became clear that the constant quasi-steady model is unphysical and the model fails to predict instability if the lift derivative is positive. Instead of a constant time delay, a memory effect was proposed in the quasi-unsteady model assuming the effect is due to the diffusion-convection process of the vorticity induced by the motion of the cylinder.

Similar to the case of tube arrays, a time delay between the lift force and the motion of an airfoil also occurs in the unsteady aerodynamics theory. A great effort of research has been dedicated to this phenomenon. The Wagner's indicial function (Wagner, 1925) and the Theodorsen function (Theodorsen, 1934), which have been widely used for over three-quarters of a century, described the time delay in the time domain and the frequency domain, respectively. Several researchers extended these models to bluff bodies such as bridge decks (R. H. Scanlan, 1996), square-section cylinders (Luo & Bearman, 1990) by reformulating and adapting the time delay function. Significant successes have been achieved in this extension of unsteady aerodynamics theory. It is, therefore, reasonable to expect that the unsteady aerodynamics theory should be applicable to cylinders in tube arrays to study the time delay.

CHAPTER 3 ARTICLE 1: DEVELOPMENT OF A TIME DELAY FORMULATION FOR FLUIDELASTIC INSTABILITY MODEL

Li H. and Mureithi N. W (2016) submitted to Journal of Fluids and Structures (10th June 2016).

Abstract

Tube arrays in industrial components such as heat exchangers and steam generators are susceptible to damage due to fluidelastic instability (FEI). In the present work a new time delay formulation for the quasi-steady FEI model is derived in the frequency domain in the form of an Equivalent Theodorsen Function. Unsteady and quasi-static fluid forces were measured to determine the time delay formulation. The effect of Reynolds number on the static force coefficients was also investigated. The time delay function was found to be also dependent on the Reynolds number. Comparison to other time delay functions proposed in the quasi-steady and quasi-unsteady models is made. Using the new function, a stability analysis was carried out to predict the critical velocity for a range of mass-damping parameters and compared with other theoretical models. The results show a significant improvement over the constant time delay quasi-steady model and the quasi-unsteady model.

Key words: fluidelastic instability, Time delay, Theodorsen function, Lift coefficient, Reynolds number.

Nomenclature

$[M_s],[C_s],[K_s]$	The mass, damping and stiffness matrices of the structure, respectively
$[M_f],[C_f],[K_f]$	The added mass, damping and stiffness matrices of the fluid, respectively
$\ddot{x},\dot{x},x$	Tube acceleration, velocity, displacement vector, respectively
F_f	General form of the fluid force
ρ	Fluid density
U,U_p	Flow free stream velocity, flow pitch velocity, respectively
D	Tube diameter
λ	Complex eigenvalue
μ	The parameter of the constant time delay quasi-steady model

τ	Dimensionless time
$\Phi(\tau)$	Memory function
α_i, δ_i	Memory function parameters
$H(\tau)$	Heaviside step function
$C_D, C_L, \partial C_L / \partial \bar{y}$	Steady drag and lift coefficients, derivative of the lift coefficient with respect to the dimensionless displacement in the lift direction, respectively
k	Reduced frequency
$C(k)$	Equivalent Theodorsen Function
$F(k), G(k)$	The real part and imaginary part of $C(k)$, respectively
$A(k), \phi(k)$	The magnitude and phase of $C(k)$
C_f, ϕ_f	The magnitude and phase of the unsteady fluid force coefficient
C_{da}, C_s	Damping and stiffness coefficient, respectively
H_{Fy}	Transfer function between the unsteady fluid force and tube motion

3.1 Introduction

Tube arrays in industrial components such as heat exchangers and steam generators are susceptible to damage due to flow-induced vibration (FIV). As the name suggests, FIV is the interaction between fluids and structures that can potentially cause excessive tube vibration. The phenomenon has been studied at least since the 1970s. Significant research effort has been dedicated to FIV so that the main mechanisms are now reasonably well understood. It is generally agreed that four different vibration excitation mechanisms are normally important in heat exchanger tube arrays. These mechanisms include periodic vortex shedding or more generally, flow periodicities, random excitation caused by turbulent flow, fluidelastic instability and acoustic resonance. Fluidelastic instability (FEI), among these mechanisms, is considered to have the greatest potential for short term damage to heat exchangers.

Fluidelastic instability is a self-excitation mechanism due to the motion-dependent fluid forces. The amplitude of vibration grows once the flow velocity exceeds a critical threshold. It is well known that even a single flexible tube in an otherwise rigid tube array subjected to cross-flow may

experience large amplitude vibration due to FEI. Because of its extremely destructive nature, a considerable research effort has been undertaken over the past fifty years in an attempt to reveal the underlying mechanisms leading to fluidelastic instability. Some excellent reviews on the subject are provided by Paidoussis (1983), Price (1995),D. t. Weaver and Fitzpatrick (1988), Pettigrew and Taylor (1991, 2003a, 2003b) and Chen (1984).

Fluidelastic instability may be caused by two distinct mechanisms: the damping controlled and the stiffness controlled instability mechanisms. Damping controlled instability is governed by the velocity dependent fluid forces and takes place when the total damping switches from positive to negative. The mechanism only needs one degree-of-freedom. Stiffness controlled instability is caused by the antisymmetric stiffness term. It is also called coupled mode flutter (in aeroelasticity) since at least two modes are required such that the relative motion between tubes can produce the force needed to overcome the structural damping.

The general governing equation of motion for the tube array subjected to single-phase cross-flow can be written as

$$[M_s]\{\ddot{x}\}+[C_s]\{\dot{x}\}+[K_s]\{x\}=F_f\left(\ddot{x},\dot{x},x,\rho,U,D,\cdots\right) \tag{3.1}$$

where $[M_s],[C_s],[K_s]$ are the mass, damping and stiffness matrices of the structure, respectively. F_f is the general form of the fluid force, $\{\ddot{x}\}$ the tube acceleration vector, $\{\dot{x}\}$ the tubes velocity vector and $\{x\}$ the tubes displacement vector.

Some theoretical or semi-empirical models have been developed to predict the critical velocity for fluidelastic instability. These include the quasi-static (Blevins, 1974; Connors, 1970), quasi-steady (Price & Paidoussis, 1984), quasi-unsteady models (Granger & Paidoussis, 1996; Meskell, 2009), the analytical channel flow model (Lever & Weaver, 1982) and the unsteady model (Chen, 1987; Tanaka & Takahara, 1981). The differences between these models lie in the definitions of the dynamic fluidelastic forces which are the terms in the right hand side of the governing equation as shown in Eqn. (3.1). For example, the quasi-steady model was developed based on the position dependent steady fluid forces measured on the tubes. In the analytical channel flow model, the fluid forces are estimated directly using the unsteady Bernoulli equation. The unsteady model was developed by measuring directly the unsteady forces acting on the vibrating tubes. One of the most

important parameters among these models is the time delay, or phase lag, between the tube motion and the fluid forces generated thereby.

In the quasi-static model, it is assumed that the fluid-dynamic forces acting on the cylinder oscillating in the flow are, at any instant of time, equal to the forces on the stationary cylinders in the identical position. Compared to the experimental results, the model is, however, unable to predict the critical velocity of the single flexible tube in an otherwise rigid tube array. To overcome this difficulty, a constant time delay was introduced in the quasi-steady model by Price and Paidoussis (1986). The modified fluid force then becomes:

$$F_f = -\left[M_f\right]\{\ddot{x}\} + \left[C_f\right]\{\dot{x}\} + \left[K_f\right]e^{-\lambda\mu D/U}\{x\} \tag{3.2}$$

where $\left[M_f\right], \left[C_f\right], \left[K_f\right]$ are the added mass, damping and stiffness matrices of the fluid. λ is the complex eigenvalue. The function $e^{-\lambda\mu D/U}$, $\mu \sim O(1)$, introduces the time delay which may induce the negative damping. Price and Paidoussis postulated that the time delay is due to the retardation of flow approaching the cylinder.

Later, Granger and Paidoussis (1996) improved the quasi-steady model by replacing the constant time delay with a memory function. The important unsteady effects are then considered. The authors attributed the time delay effect to the diffusion-convection process of the vorticity induced by the motion of the cylinder. Their modified fluid force is expressed as follows:

$$F_f = -\left[M_f\right]\{\ddot{x}\} + \left[C_f\right]\{\dot{x}\} + \left[K_f\right]\{h * x\} \tag{3.3}$$

The convolution function which is in terms of the dimensionless time τ $\left(\tau = Ut/D\right)$ in Eqn. (3.3) is defined as follows:

$$h * x = \int_0^{\tau} \frac{d\Phi\left(\tau - \tau_0\right)}{d\tau} x\left(\tau_0\right) d\tau_0 \tag{3.4}$$

This introduces the memory function which is of key interest in the quasi unsteady model. The memory function $\Phi\left(\tau\right)$ which accounts for the time delay tends to 1 as $\tau \to +\infty$. The function can be approximated by a linear combination of decaying exponentials and a Heaviside step function $H\left(\tau\right)$ as follows

$$\Phi(\tau)=\left[1-\sum_{i=1}^{N}\alpha_i e^{-\delta_i \tau}\right]H(\tau) \tag{3.5}$$

It is noteworthy that the memory function forms a general framework for the foregoing models as the quasi-static model can be retrieved by setting $\alpha_i=\delta_i=0$, while the quasi-steady model is obtained by setting $\alpha_i=\delta_i=0, H(\tau)=H(\tau-\mu)$. The values for α_i and δ_i in the model were obtained using experimental data.

To investigate the flow physics underlying the time delay function proposed by Granger and Paidoussis (1996); Meskell (2009) proposed a simple wake model to demonstrate that the underlying process of vorticity transport accounts for the time delay. The time delay function proposed in the quasi-unsteady model was obtained numerically in Meskell's work.

It is evident that the memory function $\Phi(\tau)$ in Eqn. (3.5) is identical to the approximate expression of Wagner function of unsteady aerodynamics theory. Luo and Bearman (1990) applied the unsteady aerodynamics theory to estimate the fluctuating lift force induced by the transverse oscillation of a square-section cylinder. This model showed improved agreement between theory and experiment which shows that the unsteady aerodynamics theory should have a certain degree of generality and should be applicable to cylinders in tube arrays.

In unsteady aerodynamics theory both time- and frequency- domain descriptions of the aerodynamics forces acting on thin airfoils have been applied in the aeroelastic analysis models with reasonable success. Among the wide range of unsteady aerodynamics models, the classical models of Wagner (1925) and Theodorsen (1949) remain widely used for over three-quarters of a century. Wagner proposed the so-called indicial function which gives the relationship between the indicial lift force and the transient step change in angle of attack of an airfoil in an incompressible flow. Theodorsen obtained a transfer function in terms of the lift force and the motion of the airfoil under harmonic oscillations. Garrick (1938) and Jones (1938) observed that Theodorsen and Wagner functions are equivalent representations of the effect of the wake (the lift force due to circulation) in the frequency domain and time domain, respectively. The interested reader is referred to Fung (2002) for further information on these models.

These descriptions both in time-domain and frequency-domain were not only adapted to the motion-induced forces on the streamlined airfoil, but reformulated and adapted to the bluff bodies,

such as the bridge decks (Farsani et al., 2014; R. Scanlan, 2000; R. Scanlan & Jones, 1999; R. H. Scanlan, 1996) and rectangular cylinders (Hatanaka & Tanaka, 2008). In these cases, vortex shedding, flow separation, reattachment and other possible unsteady effects may occur in the flow which is not compatible with the hypothesis mentioned before. The analytical closed-form formulations for the motion-induced forces are hence not available. Nevertheless, several approaches have been developed to overcome this drawback.

In the cases of frequency-domain approaches, it is the common practice to obtain the frequency-dependent functions (namely, the flutter derivatives or aeroelastic derivatives which are similar to the Theodorsen function) by experimental means (Miranda，S, 2013). In the context of bridge decks, the aerodynamics loads acting on bridge sections were expressed in a linear form. The flutter derivatives were evaluated by harmonically forcing the deck section and extracting the derivatives via the method of least squares (Simiu & Scanlan, 1996).

As regards the time-domain approaches, great challenges exist in the experimental evaluation of the indicial function (similar to the Wagner function) due to the difficulties arising in the direct measurements of the response to step motions. Computational fluid dynamics (CFD) approaches have therefore been developed to obtain the indicial function, for instance by Farsani et al. (2014), Hatanaka and Tanaka (2008) and Braun and Awruch (2003). Scanlan (2000) first presented the relations between the indicial functions and the flutter derivatives. An indicial function for the bluff section was obtained based upon the measured flutter derivatives.

It is clear that significant successes have been achieved in the extension of unsteady aerodynamics theory. It is therefore reasonable to expect that the unsteady aerodynamics theory should be applicable to cylinders in tube arrays.

As previously noted, there is agreement on the idea of introducing a time delay in the fluidelastic instability models. However, the phenomenon behind this time delay is still subject to many possible explanations, and the physics is still not well understood. Because of the generality between the unsteady aerodynamics theory and quasi-unsteady model as aforementioned and its successful extension, the authors decided to investigate the time delay effect in the frequency domain based on the unsteady aerodynamics theory in order to shed more light on the physics of fluidelastic instability.

In the present work, the concept of an Equivalent Theodorsen Function is applied to arrive at a time delay (or equivalently phase delay) formulation in the frequency domain. To determine the time delay function, unsteady fluid forces and quasi-static force coefficients are measured in a rotated triangular tube array subjected to water flow. The resulting time delay function is then used to predict the critical velocity for fluidelastic instability. The stability results are compared with experimental data and other models to assess the validity of the proposed model.

3.2 Theoretical Model

It is well known that FEI may occur even for a single flexible cylinder in a rigid tube array subjected to cross-flow. Lever and Weaver (1986) pointed out that the single flexible tube in the rotated triangular tube array has essentially the same critical velocity as the corresponding fully flexible tube array and the dynamic instability occurs in the transverse direction. For simplicity, consideration is given here to the particular case of a single flexible tube in an otherwise rigid tube array. The tube is free to move in the transverse direction. We note, however, that the time delay function to be developed remains valid for flexible arrays with appropriate considerations for multiple degrees-of-freedom.

Considering a single flexible cylinder in a rotated triangular tube array subjected to a cross-flow and vibrating in the lift direction, the lift force per unit length can be expressed as (Granger & Paidoussis, 1996):

$$F_L = -m_a \ddot{y} - \frac{1}{2}\rho U_p D C_D \dot{y} + \frac{1}{2}\rho {U_p}^2 \frac{\partial C_L}{\partial \overline{y}} h * y \tag{3.6}$$

where m_a is the tube added mass, C_D the drag coefficient, $\frac{\partial C_L}{\partial \overline{y}}$ the derivative of the lift coefficient with respect to the dimensionless displacement in the lift direction, U_p the pitch velocity and D the tube diameter. The displacement of the tube in the lift direction y is convolved with the time delay function $h(\tau)$ to account for the time delay. Note that $y, \dot{y}, \ddot{y}$ are dimensional.

The convolution operation is defined as follows:

$$h * y = \int_{-\infty}^{\tau} \frac{d\Phi(\tau - \tau_0)}{d\tau_0} y(\tau_0)\, d\tau_0 = \Phi(0)\, y(\tau) + \int_0^{\tau} \frac{d\Phi(\tau_0)}{d\tau_0} y(\tau - \tau_0)\, d\tau_0 \tag{3.7}$$

In what follows, we propose to reformulate the time delay term of Eqn.(3.7) in the frequency domain. This is achieved via the introduction of the Equivalent Theodorsen Function. As we show later, the frequency domain representation sheds light on important characteristics of the time delay effect. Furthermore, the formulation introduces a direct link to other physical systems susceptible to fundamentally the same type of instability considered here.

Considering the commutative property of the convolution integral, the lift force in Eqn.(3.6) can be rewritten as follows:

$$F_L = -m_a\ddot{y} - \frac{1}{2}\rho U_p D C_D \dot{y} + \frac{1}{2}\rho {U_p}^2 \frac{\partial C_L}{\partial \bar{y}} \int_{-\infty}^{\tau} \Phi(\tau - \tau_0) \frac{dy(\tau_0)}{d\tau_0} d\tau_0 \tag{3.8}$$

where the lower limit of the integral is taken as $-\infty$ in order to include the instant just before the onset of tube motion. It should be recalled that $\Phi(\tau - \tau_0) = 0$, for $\tau < \tau_0$. When the tube undergoes a harmonic motion $y = y_0 e^{i\omega t}$, the convolution integral in Eqn. (3.8) becomes

$$\lim_{\varepsilon \to 0^+} ik \int_{-\infty}^{\tau} \Phi(\tau - \tau_0) e^{ik\tau_0 + \varepsilon\tau_0} d\tau_0 = C(k) e^{ik\tau} \tag{3.9}$$

where $k = \omega D / U_p$ is the reduced frequency. A convergence factor $e^{\varepsilon\tau_0}, (\varepsilon > 0)$, is introduced to avoid the mathematical difficulty of oscillatory divergence at the lower limit. Eqn.(3.9) introduces the Equivalent Theodorsen Function, $C(k)$, for a tube array. The Equivalent Theodorsen Function incorporates the effect of time delay in a frequency domain representation. The lift force in Eqn. (3.8) can be expressed as follows using $C(k)$:

$$F_L = -m_a\ddot{y} - \frac{1}{2}\rho U_p D C_D \dot{y} + \frac{1}{2}\rho {U_p}^2 \frac{\partial C_L}{\partial \bar{y}} C(k)\, y \tag{3.10}$$

$\mathrm{C(k)}$ may be expressed in polar form as

$$C(k) = F(k) + iG(k) = A(k) e^{i\phi(k)} \tag{3.11}$$

where $A(k), \phi(k)$ are the magnitude and phase of $C(k)$, respectively. $C(k)$ turns out to be identical to the Theodorsen function in aerodynamics providing the memory function $\Phi(\tau)$ is

chosen as the Wagner function of unsteady aerodynamics theory. $C(k)$ can also be expressed in the form of an exponential function.

It is noted that the memory function $\Phi(\tau)$ can be interpreted as the step response of the tube motion in the tube array. The quasi-steady model with constant time delay is obviously unphysical. Many experimental challenges are posed by direct measurements of the step response in time domain. This issue can be resolved in the frequency domain using the Equivalent Theodorsen Function proposed above. To determine the Equivalent Theodorsen Function, the method is presented below.

As suggested by Sawadogo and Mureithi (2014a), it is more accurate to extract the time delay from the experimentally measured forces. Therefore, measured unsteady fluid forces are employed in this work to determine the Equivalent Theodorsen Function.

When a harmonic motion $y_0 e^{i\omega t}$ is applied to the tube, the measured unsteady fluid force may be expressed as follows (Sawadogo & Mureithi, 2014a) :

$$F_{uns} = \left\{ \frac{1}{2} \rho U_p{}^2 C_f e^{i\phi_f} \right\} y_0 e^{i\omega t} = \left\{ \omega^2 m_a + i\omega \frac{\rho U_p D}{2} C_{da} + \frac{\rho U_p{}^2}{2} C_s \right\} y_0 e^{i\omega t} \tag{3.12}$$

where C_f and ϕ_f are the unsteady fluid force coefficient magnitude and phase, m_a, C_{da} and C_s are fluid added mass, damping coefficient and stiffness coefficient, respectively.

The Equivalent Theodorsen Function is determined by equating the unsteady fluid force expression of Eqn. (3.12) to the quasi-steady fluid force expression of Eqn. (3.10). This yields

$$\begin{aligned} G(k) &= k\left(C_{da} + C_D\right) \Big/ \frac{\partial C_L}{\partial \bar{y}} \\ F(k) &= C_s \Big/ \frac{\partial C_L}{\partial \bar{y}} \end{aligned} \tag{3.13}$$

and

$$\begin{aligned} A(k) &= \sqrt{F(k)^2 + G(k)^2} \\ \phi(k) &= \tan^{-1} \frac{G(k)}{F(k)} \end{aligned} \tag{3.14}$$

Eqn. (3.13) and Eqn. (3.14) express the relation between Equivalent Theodorsen Function and the fluid force coefficients (both the quasi-static force coefficients and unsteady force coefficients). These fluid force coefficients are also important parameters of the unsteady model and quasi-steady model. The Equivalent Theodorsen Function may be extracted as long as the force coefficients are known. Consequently, experimental tests were conducted to determine the unsteady and static force coefficients.

3.3 Experimental Test

3.3.1 Test loop and test section

A schematic of the flow loop, including the test section, is shown in Figure 3-1. The flow loop consists of a centrifugal pump used to pump the water through the test section and back to the water tank at a maximum flow rate of 26 l/s. The water flow rate is measured by a magnetic flowmeter (MAG500). All measurements were conducted at room temperature (approximately 22 ℃).

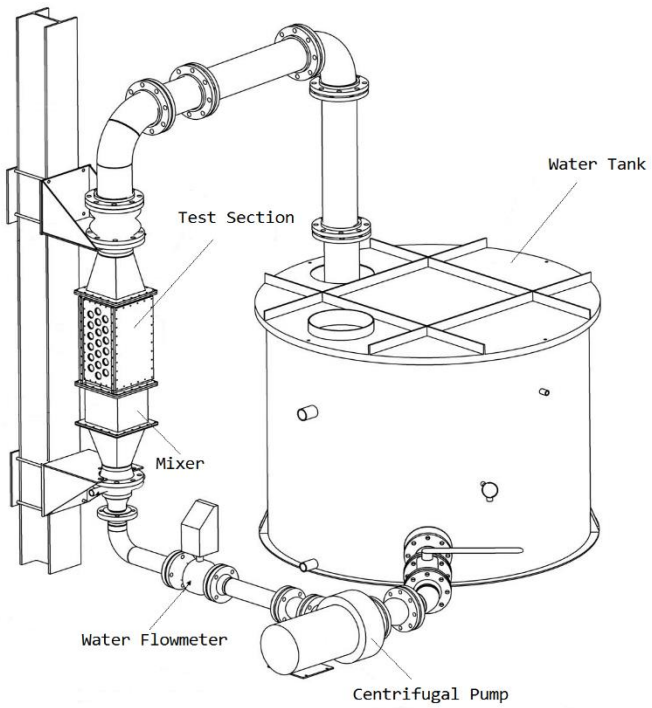

Figure 3-1 : Test Loop.

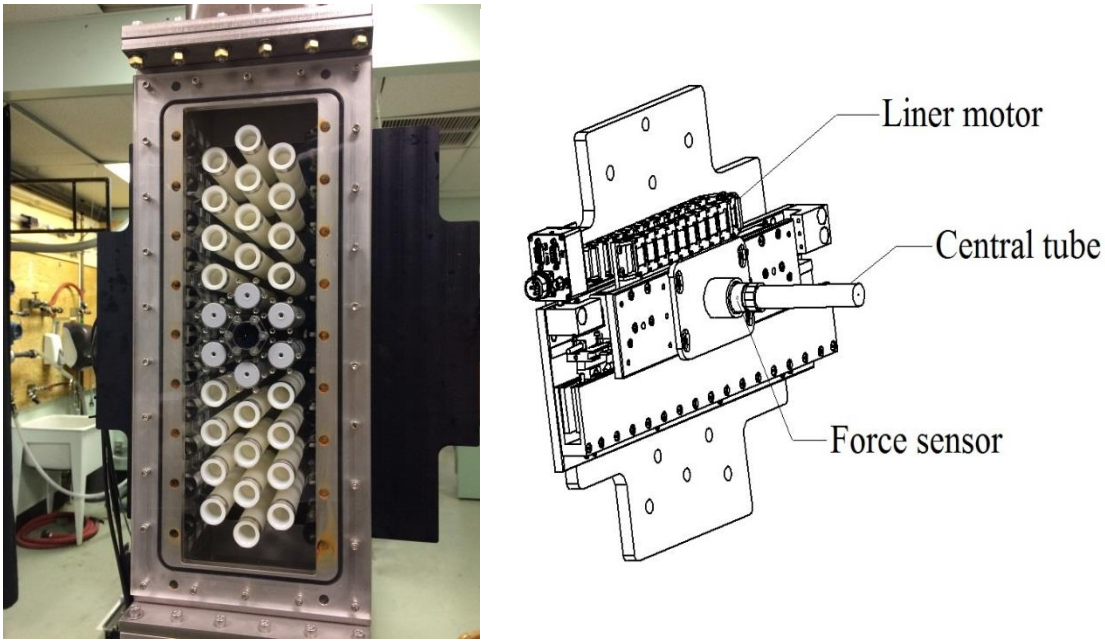

(a) (b)

Figure 3-2 : Test Section and Displacement Mechanism: (a) Test section of a Rotated Triangular Tube Array, (b) Central Tube Mounted on the Linear Motor.

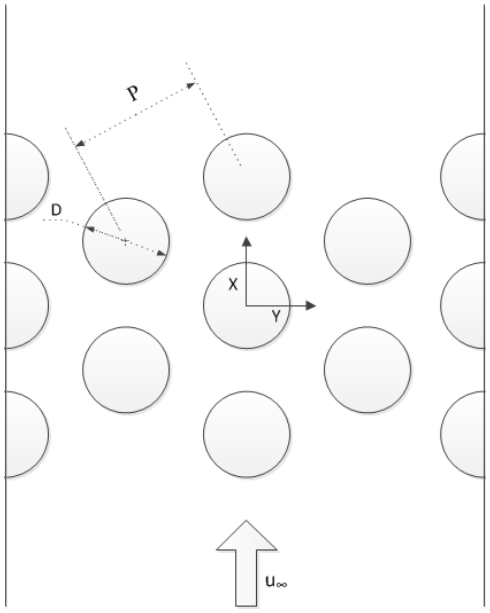

Figure 3-3 : Tube array configuration

The test section, shown in Figure 3-2 (a), measures 470mm in length with a cross-section area of $0.01613\ \mathrm{m}^2$. The array under test is a rotated triangular tube array with a pitch ratio of 1.5 as shown in Figure 3-3. The central tube, made of aluminum, is mounted on an ATI Nano25 force transducer attached to a displacement system as shown in Figure 3-2 (b). The resolution of the force transducer is 0.04 N. The linear motor (Parker Trilogy Ironless Positioner) used in the displacement system is able to deliver up to 3000N of peak force and 660N of continuous force. It allows the central tube to be displaced in the transverse direction at tube excitation frequencies up to 24 Hz in water flow. The other tubes in the array including 30 tubes and 22 half tubes are rigid and made of Polycarbonate. Half tubes are attached to the wall to reduce the wall effect. The tubes are 22 mm in diameter and 137.7 mm in length.

3.3.2 Test Procedure

The unsteady fluid force measurements were conducted in the lift direction for up to 9 different velocities varying from 0.2 m/s to 1.4 m/s. For each velocity, 11 different excitation frequencies varying from 6 Hz to 24 Hz were applied to the central tube. The excitation amplitude was 2 mm (0.09D). The fluid force and displacement data were acquired at a sampling rate of 2000 Hz and the acquisition time was adjusted according to the excitation frequency. For lower than 12 Hz excitation, the acquisition time is 300 s. It is 240 s for 12-18 Hz and 180 s for 18 Hz-24 Hz. The added mass was measured in still water and relatively high frequencies.

As noted above the measured unsteady fluid forces may be expressed as shown in Eqn. (3.12) To determine the force coefficients from experiments, a transfer function between the fluid force and the displacement of the vibrating tube is defined as follows:

$$H_{Fy} = \frac{F_f}{y_0 e^{i\omega t}} \tag{3.15}$$

The fluid force magnitude and phase are given therefore by

$$C_f = \frac{\sqrt{\Re\left(H_{Fy}\right)^2 + \Im\left(H_{Fy}\right)^2}}{\frac{1}{2}\rho U^2}$$
$$\phi_f = \tan^{-1}\left(\frac{\Im\left(H_{Fy}\right)}{\Re\left(H_{Fy}\right)}\right) \tag{3.16}$$

The quasi-static fluid force measurements were conducted in the same test setup. For a given velocity, finite displacements in increments of 0.5mm (0.023D) were applied to the central tube using the displacement system. The sampling frequency of fluid force data acquisition is 2000 Hz. At each position lift and drag forces were measured under steady flow conditions and each measurement was averaged over 120 s. To examine the effect of Reynolds number on the steady drag coefficients and the lift coefficient derivatives, the measurements of quasi static forces were also carried out for 9 different velocities. For each flow condition, at least 3 different measurements were taken and averaged.

3.4 Results and Discussions

3.4.1 Force coefficients

The results of the unsteady fluid force measurements are presented in Figure 3-4 and Figure 3-5. The pitch velocity U_P was used to render the force coefficients according to Eqn.(3.12). The magnitude and phase results of the unsteady fluid force coefficient in the lift direction are presented as functions of the reduced velocity U_p / fD. The solid line obtained by analytical curve fitting is applied to highlight the data trend. It can be seen that the unsteady fluid forces are strongly dependent on U_p / fD. Both the magnitude and phase data seems to fit well to the trend line, although the phase data shows some scatter at higher U_p / fD. The phase increases with U_p / fD up to around $U_p / fD = 5$ and then decreases toward negative values.

Figure 3-6 shows the drag coefficient as a function of the tube displacement for a range of Reynolds numbers. It is clear that the effect of the tube displacement in the transverse direction on C_D is negligible. The lift derivative variation with tube displacement for a range of Reynolds number is shown in Figure 3-7. The results of at least three different tests are shown in each case. The lift coefficient is zero at the central position and increases in magnitude with tube displacement. At least three different measurements were taken and averaged to obtain the averaged lift derivative.

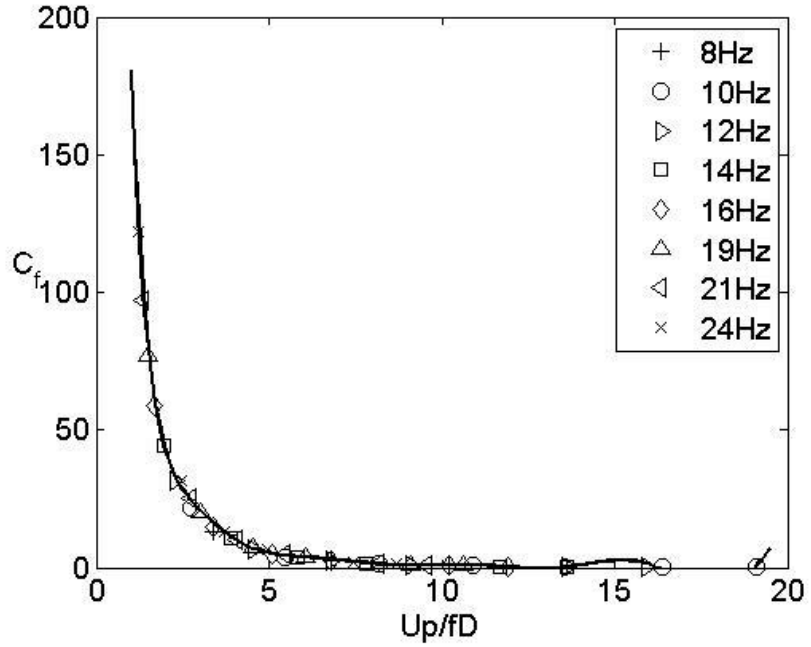

Figure 3-4 : Magnitude of unsteady fluid force coefficient versus U_p / fD .

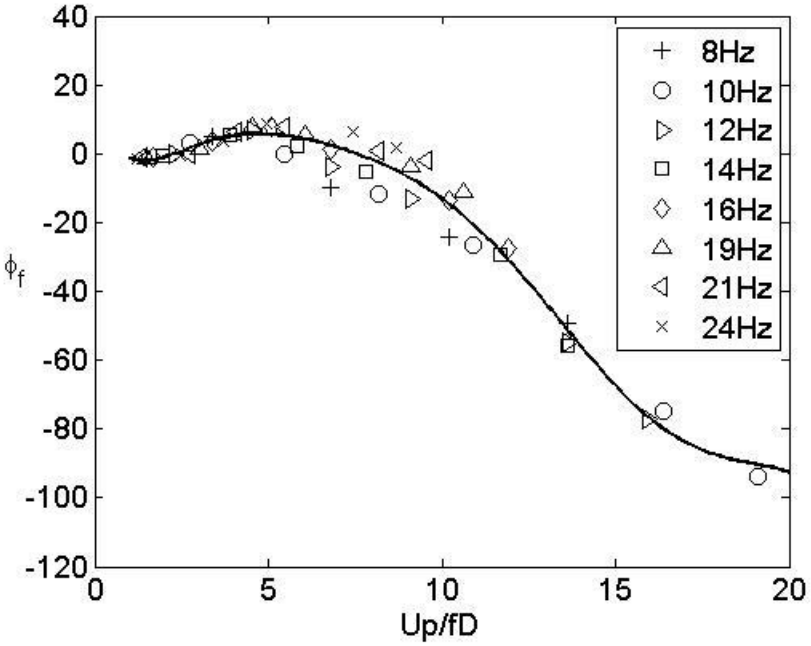

Figure 3-5 : Phase of unsteady fluid force coefficient versus U_p / fD .

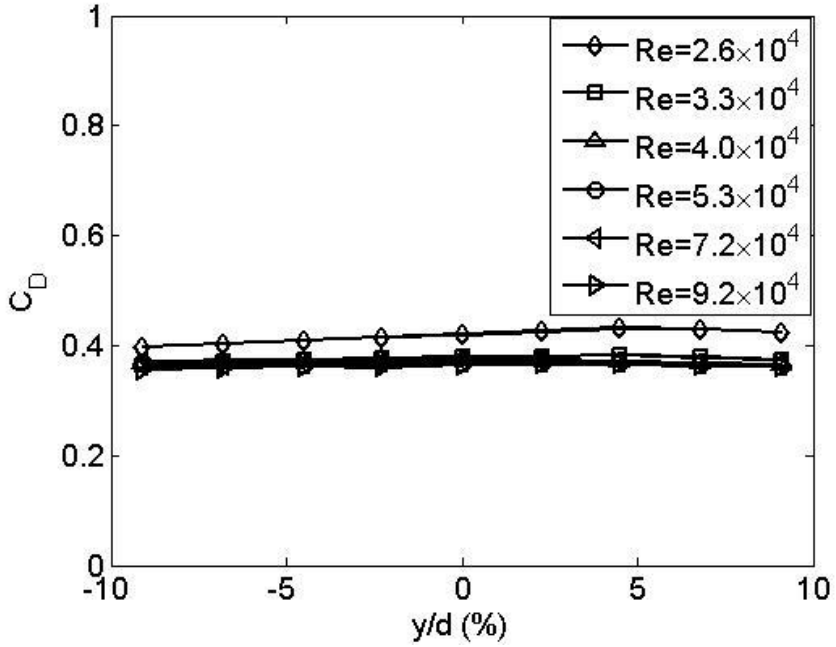

Figure 3-6 : Drag coefficient variation with tube displacement.

The drag coefficient and derivative of the lift coefficient as functions of Reynolds number are presented in Figure 3-8 and Figure 3-9. The drag coefficient decreases dramatically with increasing Reynolds number but approaches a nearly constant value at high Reynolds number. The derivative of the lift coefficient, on the other hand, strongly depends on Reynolds number. It increases quasi-linearly with Reynolds number (flow velocity) and the sign changes from negative to positive at around $\mathrm{Re} = 8\times10^4$ suggesting that the flow around the tube undergoes an important change near this Re. It is the fundamental change in the flow distribution around the tube that causes the change of lift coefficient. It is well known that the lift derivative is important for FEI theoretical model. The results here imply that fluidelastic instability may be strongly dependent on Reynolds number.

In past research, the effect of Reynolds number on the force coefficients has often been neglected (Sawadogo & Mureithi, 2014b). Sawadogo and Mureithi (2014a) measured the lift derivative in the water flow in a rotated triangular tube array of the same pitch ratio for $\mathrm{Re} = 8.4\times10^4$. The measurements are consistent with the results obtained here. Mahon and Meskell (2012) obtained the lift derivative by measuring the surface pressure on the central tube in a rotated triangular tube array with the pitch ratio of 1.375. It was found that the lift derivative decreases with increasing Reynolds number but the trend changes and the derivative becomes positive at high Reynolds

number. This change in the trend is found to coincide with a change in the flow behavior. The authors attributed this change to jet switching in the tube array. Charreton et al. (2015) studied the lift derivative for low Reynolds numbers ($\mathrm{Re} \leq 800$) in a rotated triangular tube array with $P/D = 1.5$. They found that the derivative crosses zero from negative values at around $\mathrm{Re} = 200$ and reaches an asymptote for higher values. It was suggested that the lift derivative is sensitive to the tube array pattern, pitch ratio and Reynolds number. Presently, reported work on the lift derivative remains limited in the open literature. Future work is clearly needed to fully understand this dependence on Re.

3.4.2 Equivalent Theodorsen function

During the past 50 years, several theories, as outlined before, have been developed to predict FEI of tube arrays in cross-flow. The general conclusions obtained from the various theoretical models mostly agree. In particular, it is shown that, in order to predict single degree-of-freedom FEI, the time delay between the tube motion and the fluid forces is the most important parameter to consider, no matter which theoretical model is applied with the exception of the general unsteady model which implicitly includes a phase lag.

Physically, the mechanism of time delay may be described as follows: tube motion disturbs the flow field in the neighborhood of the tube. A perturbation in the fluid force acting on the tube is therefore induced and decays continuously with time as the vorticity is transported downstream. A new steady state is attained after the vorticity has been conveyed far away from the tube by the mean flow. This typical transition between two steady states is not instantaneous but takes some time to develop.

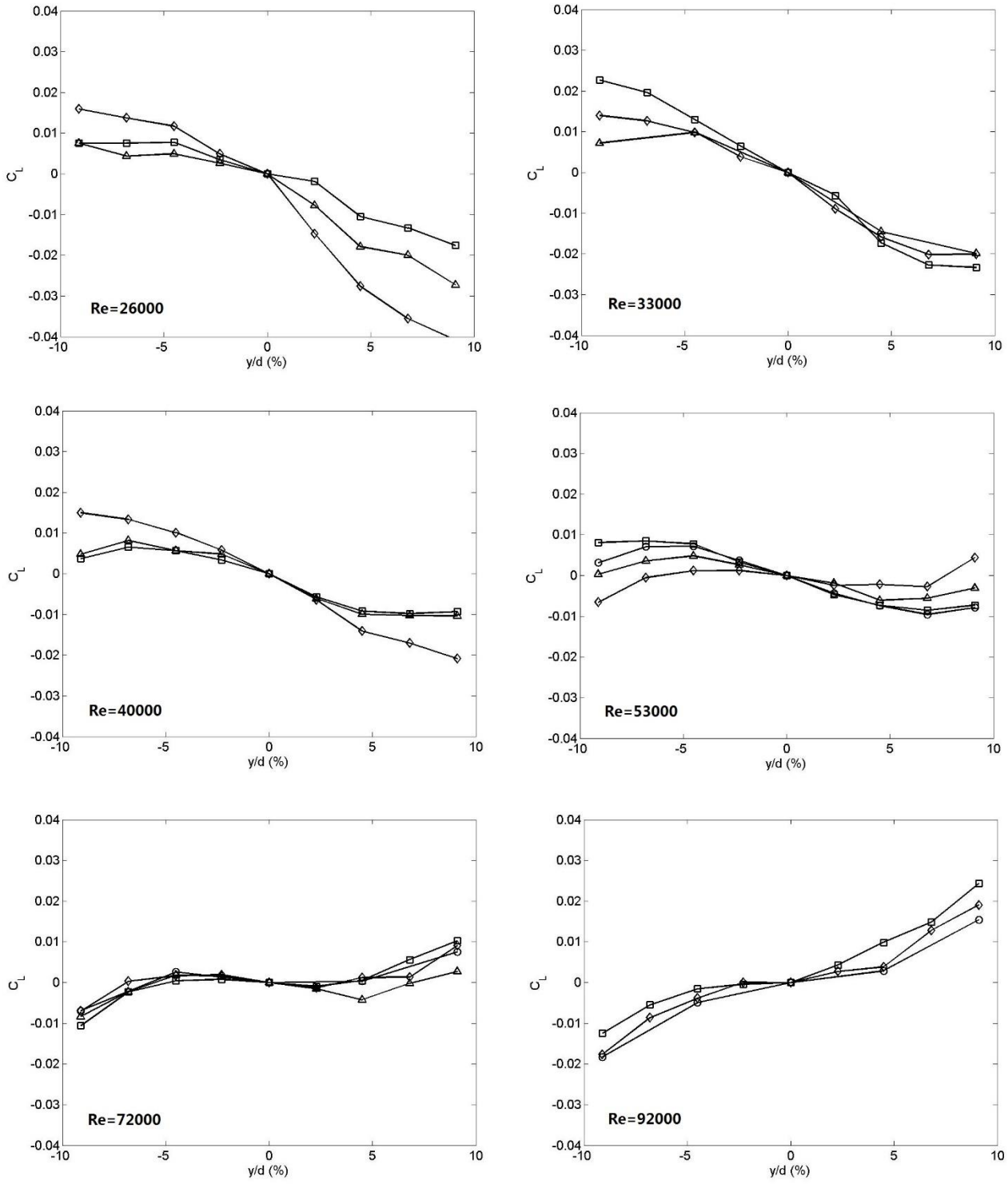

Figure 3-7 : Lift coefficient variation with tube displacement for a range of Reynolds numbers.

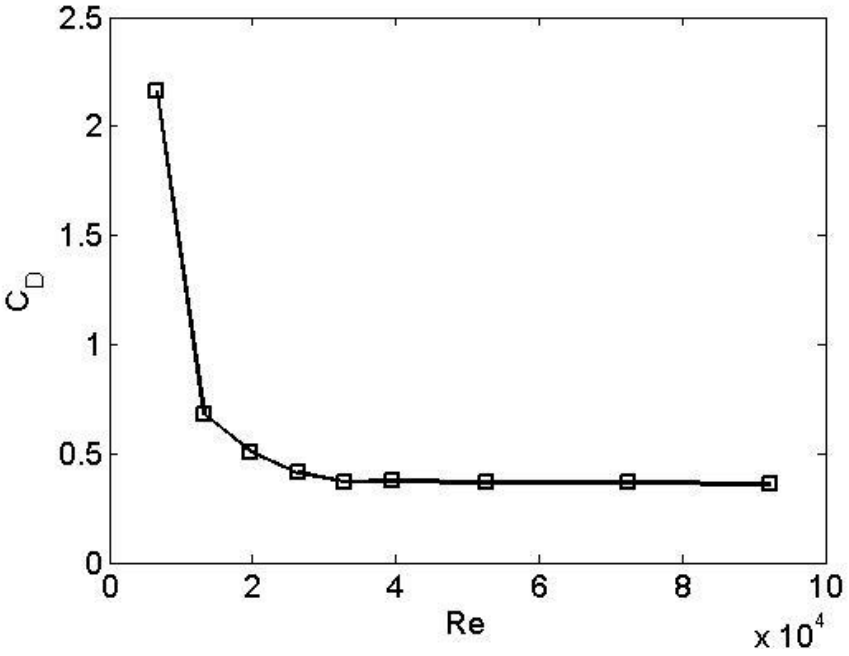

Figure 3-8 : Drag coefficient versus Reynolds number.

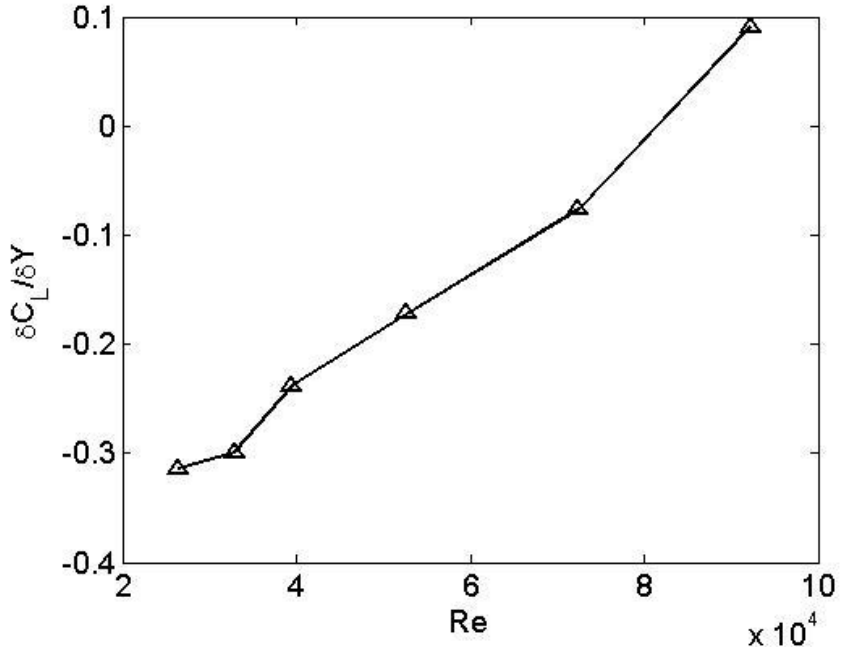

Figure 3-9 : Lift coefficient versus Reynolds number.

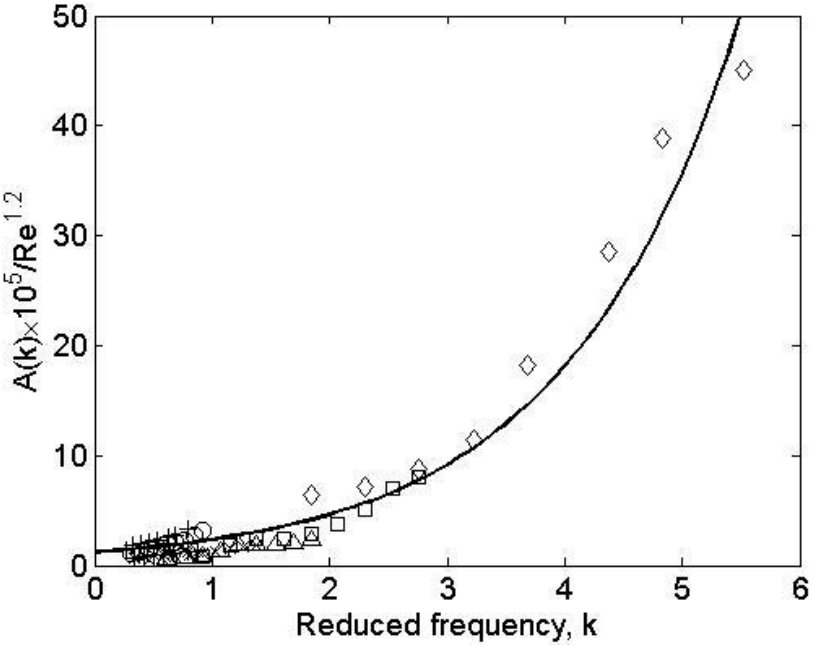

Figure 3-10 : Amplitude of the time delay function against k and Re.

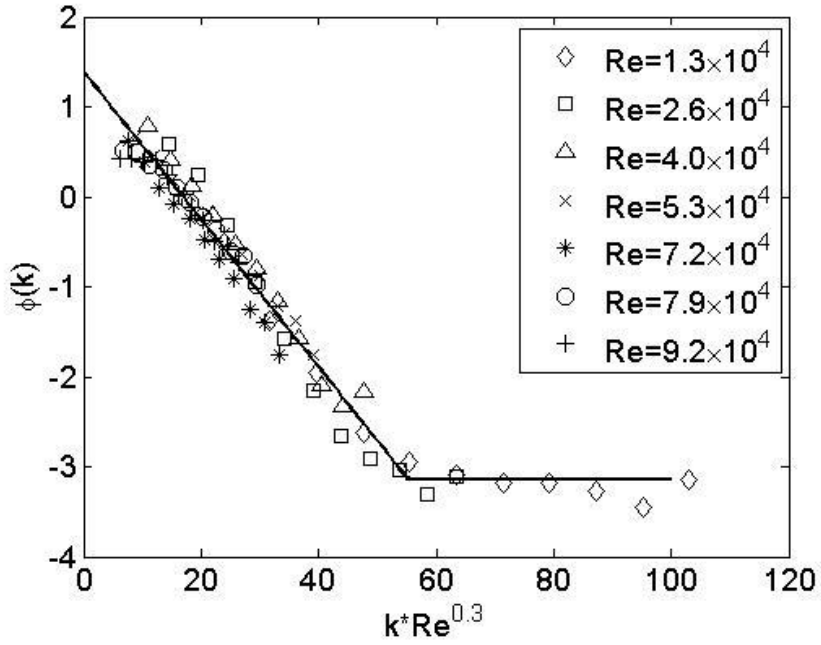

Figure 3-11 : Phase of the time delay function against k and Re.

According to Eqns. (3.13) and (3.14), once the unsteady fluid forces and static force coefficients are measured, the Equivalent Theodorsen Function can be determined in the form of a complex exponential function. Using the force data presented in Figure 3-4 and Figure 3-8, the

corresponding Equivalent Theodorsen Function was determined. This exponential function in the form of amplitude and phase with a Reynolds effect correlation is proposed and presented in Figure 3-10 and Figure 3-11. The correlations for the Equivalent Theodorsen Function amplitude and phase are given in Eqn. (3.17) and Eqn. (3.18). The amplitude and phase data collapse well onto a single trend line which indicates that the effect of Reynolds number on the time delay can be modelled and should not be ignored. Due to the limitations of the test loop, the effect of higher Reynolds numbers is not studied in the present work. Therefore, the correlations presented below are recommended for $\mathrm{Re} \le 9.2\times10^4$.

Amplitude:

$$A(k, Re) = \frac{1.189\,\mathrm{Re}^{1.2}}{10^5} e^{0.6805k} \tag{3.17}$$

Phase:

$$\phi(k, Re) = \begin{cases} -0.082k \times Re^{0.3} + 1.382; k \times Re^{0.3} \le 55 \\ -\pi; k \times Re^{0.3} \ge 55 \end{cases} \tag{3.18}$$

3.4.3 Time delay model comparison

In the quasi-steady model, the time delay was accounted for by the term $e^{-i\mu\omega D/U_p}$ inserted in the fluid force equation. In the present work this term is replaced by the Equivalent Theodorsen Function $C(k)$ or $A(k)e^{i\phi(k)}$. For combination of Reynolds number and reduced frequency corresponding to $A(k) \approx 1$ in Eqn. (3.17), the time delay term (the phase term) turns out to be the same as that proposed in quasi-steady model. In Figure 3-12 the phase data $\phi(k, Re)$ of the Equivalent Theodorsen Function is plotted as a function of reduced frequency for several Reynolds numbers. The phase related to the time delay proposed in the quasi-steady model with $\mu = 2$ is also presented for comparison (see the solid line in Figure 3-12). It can be seen that using this value $\mu = 2$ results in good agreement between the quasi-steady theory and the Equivalent Theodorsen Function-based model. This suggests that the quasi-steady model is capable of capturing the characteristic of the time delay in a certain parameter range, where the reduced frequency and

Reynolds number meet the requirement that $A(k) \approx 1$. The result also suggests that the model proposed here forms a general framework of the quasi-steady model.

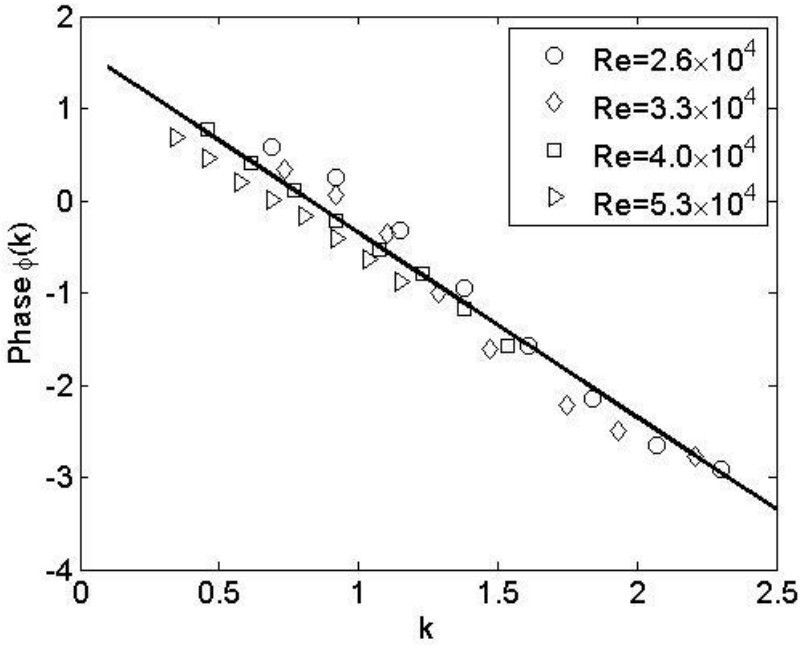

Figure 3-12 : Phase of the time delay function against k.

For the convenience of comparing the Equivalent Theodorsen Function $C(k)$ with the memory function $\Phi(\tau)$ proposed in the quasi-unsteady model, the following equivalence is established by comparing Eqn. (3.10) to Eqn. (3.7).

$$C(k) = \Phi(0) + \mathcal{F}\left(\Phi'(\tau)\right) \tag{3.19}$$

where

$$\mathcal{F}\left(\Phi'(\tau)\right) = \int_0^{\tau} \frac{d\Phi(\tau_0)}{d\tau_0} e^{-ik\tau_0} d\tau_0 \tag{3.20}$$

is the Fourier transform of the first derivative of the memory function $\Phi(\tau)$.

If the four constant parameters $\alpha_1, \alpha_2, \delta_1, \delta_2$ in Eqn. (3.5) are given and knowing that the Fourier transform of $e^{-\delta\tau}$ is $1/(\delta + ik)$, the functions $F(k)$ and $G(k)$ may be approximated as follows

$$F(k) = 1 - \alpha_1 - \alpha_2 + \frac{\alpha_1 \delta_1^{\,2}}{\delta_1^{\,2} + k^2} + \frac{\alpha_2 \delta_2^{\,2}}{\delta_2^{\,2} + k^2}$$
$$G(k) = -k\left(\frac{\alpha_1 \delta_1}{\delta_1^{\,2} + k^2} + \frac{\alpha_2 \delta_2}{\delta_2^{\,2} + k^2} \right) \qquad (3.21)$$

Eqn. (3.21) is an explicit relation between $C(k)$ and the parameters of $\Phi(\tau)$.According to this equation, the parameters of the memory function $\Phi(\tau)$ may be determined from the Equivalent Theodorsen Function proposed in the present work and vice-versa using the appropriate reciprocity relations. After extracting the values of $F(k)$ and $G(k)$ experimentally using Eqn. (3.13), the constant parameters $\alpha_1, \alpha_2, \delta_1, \delta_2$ were determined using the least-square minimization procedure.

Figure 3-13 shows the effect of Reynolds number on the memory function derived from the Equivalent Theodorsen Function model. The time delay is found to be significantly dependent on Reynolds number. Unlike the classical Wagner function, a significant initial overshoot occurs in the memory function. The overshoot strength seems to be proportional to the Reynolds number. It is important to note that the mechanism involved in the classical Wagner's model is quite different from the present model. Wagner's model is built on the assumption of fully attached flow. The memory function is therefore very different from the indicial response of an airfoil.

As mentioned earlier, the unsteady aerodynamics theory has been extended to many other physical systems such as bridge decks and rectangular cylinders. Significant successes have been achieved. The overshoot has been found to exist generally in the indicial functions of bluff bodies. Turbelin and Gibert (2002) used a computational fluid dynamic analysis to derive the lift indicial function for bluff bodies. The aerodynamic flow field indicated that the overshoot is related to the flow separation and the growth of the separation bubble from the leading edge. The bubble increases in length as the time advances. Accordingly, the lift force increases and overshoots its steady value with the growth of the bubble. After the bubble passes over the body and is shed into the downstream wake, the lift force decreases to the static value. Given the detailed research on the flow and the generality in the aerodynamics and fluid dynamic theories of airfoils, bluff bodies and tube arrays, it is reasonable to believe that it is the same fundamental phenomenon in the flow that

causes the overshoot in the memory function. The flow bubble size and the separation point position may be affected by the Reynolds number which causes the different strengths of the overshoot.

A comparison with other memory functions for the quasi-steady and quasi-unsteady models is presented in Table 3-1. The corresponding transient behaviors are also shown in Figure 3-14. In the first order quasi-unsteady model, the flow takes much longer to attain the steady state compared to the current model and the quasi-steady model. In the quasi-steady model, after a constant time delay a new steady state is reached instantaneously from the previously steady state. This is clearly unphysical.

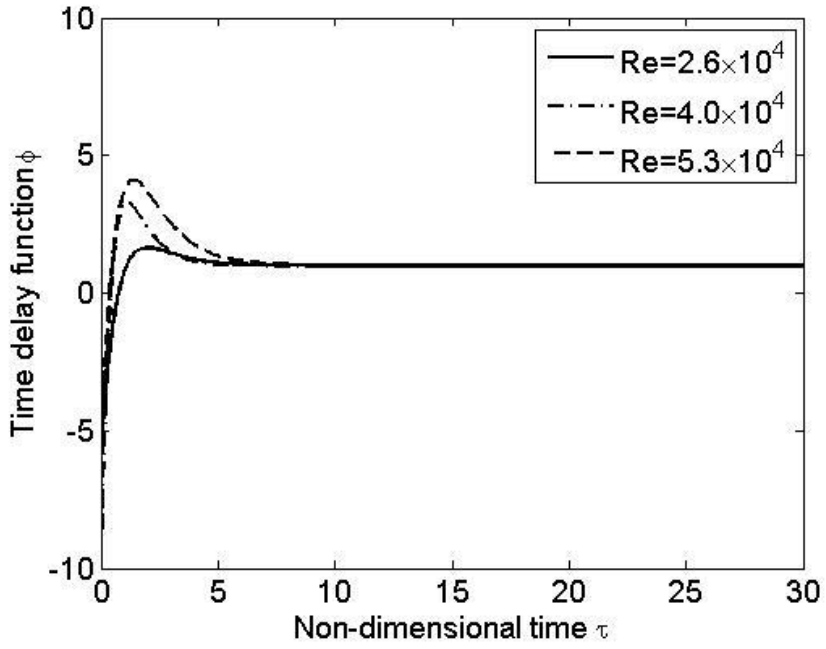

Figure 3-13 : The effect of Reynolds number on the memory function.

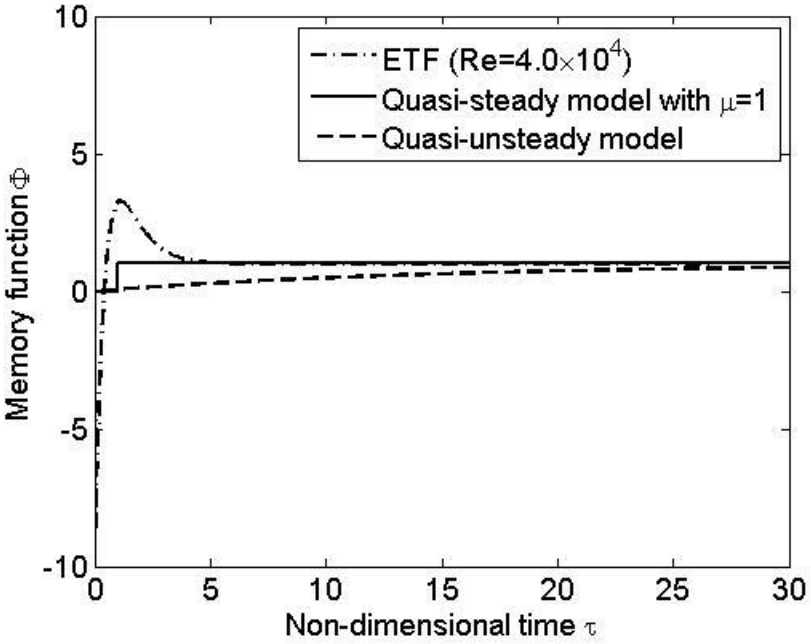

Figure 3-14 : Comparison with different memory functions for rotated triangular tube array with P/D=1.5.

Table 3-1 : Comparison with different memory functions for rotated triangular tube array with P/D=1.5. Q-S=Quasi-Steady model; Q-Unst=Quasi-Unsteady model; ETF=Equivalent Theodorsen function

Model	α_1	δ_1	α_2	δ_2
Quasi-steady model with $\mu = 1$	0	0	0	0
Quasi-unsteady model (first-order)	1	0.066	0	0
ETF ($\mathrm{Re} = 2.6\times10^4$)	-60.6	1.06	67.8	1.162
ETF ($\mathrm{Re} = 4.0\times10^4$)	-28	1.3	40	2
ETF ($\mathrm{Re} = 5.3\times10^4$)	-20	0.8	28	1.5

3.4.4 Stability analysis

In this section the performance of the Equivalent Theodorsen Function is evaluated via the stability analysis of a single flexible tube in an otherwise rigid array.

Considering a single flexible tube vibrating in the lift direction and taking into account Eqn. (3.1) and Eqn. (3.10), the equation of tube motion may be written as

$$m_s\ddot{y} + c_s\dot{y} + k_s y = -m_a\ddot{y} - \frac{1}{2}\rho U_p DC_D\dot{y} + \frac{1}{2}\rho U_p{}^2\frac{\partial C_L}{\partial \overline{y}}C(k)\,y \tag{3.22}$$

It may be rewritten in a simplified form as follows:

$$m\ddot{y} + c\dot{y} + ky = 0 \tag{3.23}$$

where

$$\begin{aligned} m &= m_s + m_a \\ c &= c_s + \frac{1}{2}\rho U_p DC_D \\ k &= k_s - \frac{1}{2}\rho U_p{}^2\frac{\partial C_L}{\partial \overline{y}}C(k) \end{aligned} \tag{3.24}$$

The eigenvalue problem associated with the equation of tube motion above may be expressed in matrix form as:

$$\det\left(\begin{bmatrix} m & 0 \\ 0 & -k \end{bmatrix} - \lambda\begin{bmatrix} 0 & m \\ m & c \end{bmatrix}\right) = 0 \tag{3.25}$$

To predict the critical instability velocity, the fluid velocity is incrementally varied. A standard iterative method is applied to solve the velocity dependent eigenvalue problem to assess the system stability. The critical velocity can be determined when the real part of at least one of the eigenvalues crosses zero.

Figure 3-15 shows a comparison of the experimental fluidelastic instability data to the predicted stability boundary using the current model and also the quasi-unsteady model. As noted earlier the Equivalent Theodorsen Function is only valid for single phase and $\mathrm{Re} \le 9.2\times10^4$, For water flow, the mass damping parameter is therefore limited to $m\delta/\rho D^2 \le 1$. A close-up view of the comparison for low mass ratio is presented in Figure 3-16. The available experimental data found

in literature come from rotated triangular tube arrays with different pitch ratio varying from 1.375 to 1.73 and subjected to water and air flow. It appears that there is significant scatter in the available experimental data. It is, however, well known that the critical velocity is also a function of tube array pitch ratio. It is therefore preferable to compare with the experimental data provided by Sawadogo and Mureithi (2014b) and Violette (2006) as they are based on the same tube array and pitch ratio and for water flow; these data are shown by solid symbols. The agreement between the current theory and experiments is fairly good. The quasi-unsteady model for the rotated triangular tube array gives the parameters of first-order time delay formulation as $\alpha_1 = 1.0, \delta_1 = 0.066$. The stability threshold obtained using the model is also plotted in Figure 3-15 and Figure 3-16 for comparison. It is found that the first-order quasi-unsteady model overestimates the critical velocity in the given range of mass damping parameter. The current model was also compared to the quasi-steady model with constant time delay ($\tau = \mu D/U, \mu = 1$). However, the latter model failed to predict instability in this range of mass damping parameter. The results suggest a significant improvement over the constant time delay quasi-steady and the quasi-unsteady models.

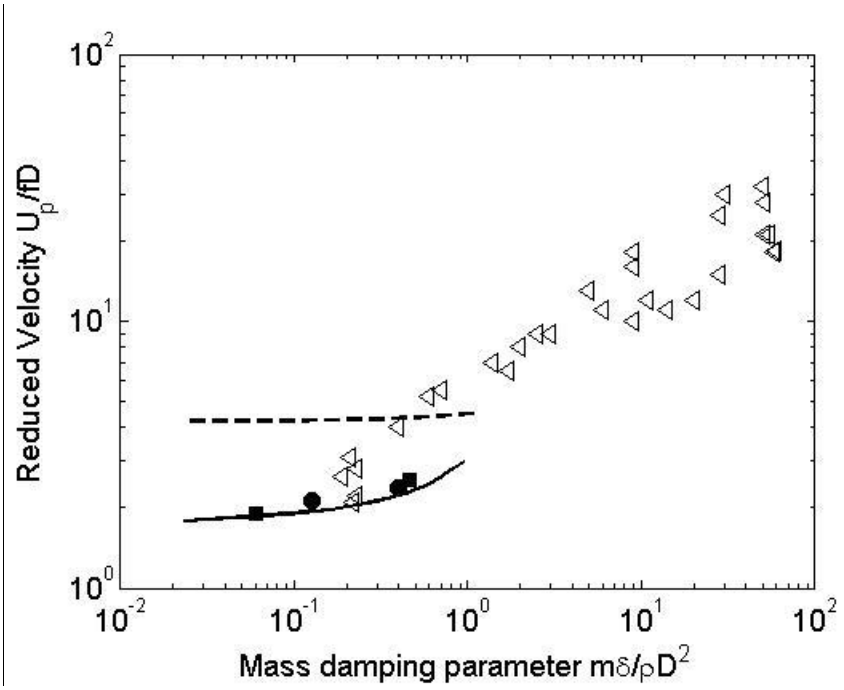

Figure 3-15 : Stability threshold for rotated triangular tube arrays. ◁, experiment data from (D. t. Weaver & Fitzpatrick, 1988); ■, experiment data from (Sawadogo & Mureithi, 2014b); ●, experiment data from (Violette et al., 2006); −− , Quasi-unsteady model; − , Current model

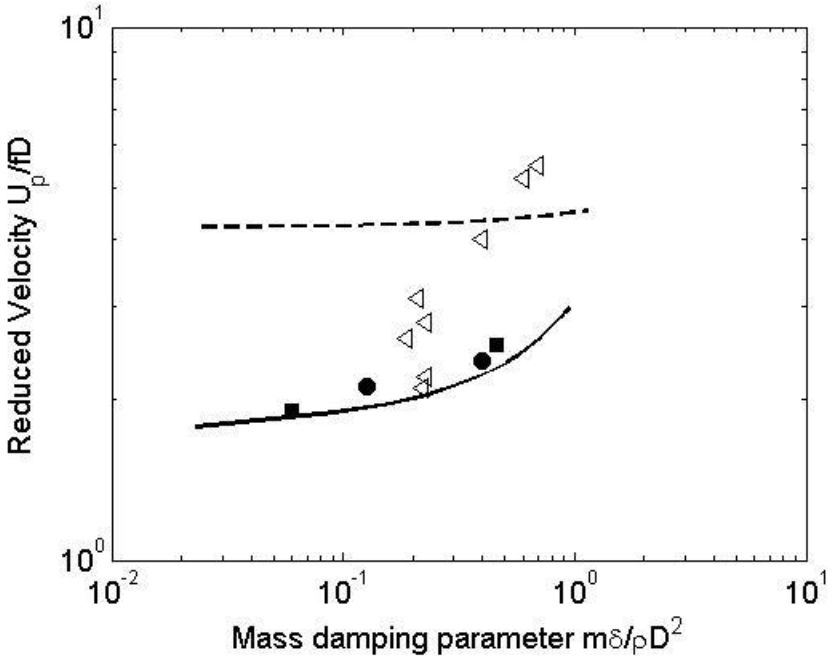

Figure 3-16 : Local stability threshold. ◁, experiment data from (D. t. Weaver & Fitzpatrick, 1988); ■,experiment data from (Sawadogo & Mureithi, 2014b); ●, experiment data from (Violette et al., 2006); −−, Quasi-unsteady model; −, Current model.

3.5 Conclusions

A new time delay formulation for the class of quasi-steady fluidelastic instability models has been proposed in the present work. The time delay formulation was derived in the form of an Equivalent Theodorsen Function.

The time delay formulation was determined experimentally and compared with other time delay functions found in the quasi-steady and quasi-unsteady models. An initial overshoot in the lift force was observed for the present model. The overshoot has also been reported for other fluid-structure interaction problems involving bluff bodies. The time delay model was found to be dependent on Reynolds number which implies that the fluidelastic instability is also Reynolds number dependent.

A stability analysis using the new time delay formulation was presented and compared to the quasi-steady and quasi-unsteady models as well as experimental data. The predicted stability threshold

compares reasonably well with experimental data and shows a significant improvement over the other models in the range of mass-damping parameters where the model is valid.

The foregoing stability analysis results confirm the validity of the model and give some confidence in the reliability of the method. The reader should remember that the time delay formulation is obtained from experiments on a rotated triangular tube array with a pitch ratio of 1.5 subjected to single-phase cross-flow. The Equivalent Theodorsen Function correlation obtained is therefore only applicable to the rotated triangular tube array with pitch ratio of 1.5 and valid for the range of Re considered. However, the method itself is more generally applicable to the other tube arrays.

CHAPTER 4 INVESTIGATION OF REYNOLDS NUMBER EFFECT ON FORCE COEFFICIENTS BASED ON CFD

As discussed in Chapter 3, the effect of Reynolds number on the force coefficients in the tube array, especially the lift coefficient, has often been neglected. It was usually assumed that the force coefficients approach constant values at high Reynolds number. The recent research reported by Mahon and Meskell (2012) and in the present work, however, indicates that the effect of Reynolds number on the lift coefficient in the rotated triangular tube array may not be ignored. Charreton et al. (2015) found that the lift coefficient is sensitive to the tube array pattern, pitch ratio and Reynolds number. Therefore, more work is clearly needed to fully understand this dependence on Re.

In this section, a numerical method (CFD) will be used to study the effect of Reynolds number on the force coefficients in the rotated triangular tube array. The turbulence models will be reviewed and described briefly. A rotated triangular tube array with a pitch ratio of 1.5 will be applied as the computational domain. The central tube was displaced with a typical value of 1.5mm (0.068D). Two cases of different velocities will be analyzed. Note that the objective of the CFD work is to investigate the Reynolds number effect on the lift derivative coefficient, the displaced tube is static and undergoes no vibration.

4.1 Turbulence model

Turbulence has a strong effect on the characteristics of the drag and lift forces of the central tube in the tube array. The flow is inherently random, three-dimensional and unsteady. Due to the complicated geometry, the flow in the tube array will be continuously separated and mixed and vortices will also be generated, so the turbulence not only comes from the flow, but also from the structure. Such turbulence consists of a wide range of spatial and time scales. It is difficult to computationally and accurately resolve all these scales. However, it is important to account for these turbulence effects in computational fluid dynamics (CFD) by using various approximated turbulence models. Until now, many advanced turbulence models in the form of one-equation, two-equation and Reynolds stress models have been developed. The most widely used models are Reynolds-averaged Navier-Stokes (RANS) models which are based on time-averaged equations. These RANS models filter out all turbulent scales from the simulation because of the time

averaging, and the effect of turbulence on the mean flow is then re-introduced through appropriate modeling assumptions. The two equation ($k-\omega$ and $k-\varepsilon$) models and the shear-stress transport (SST) model have become the most widely employed models in the flow analysis.

However, it has become clear that RANS models inherently cannot resolve certain classes of complex turbulent flow problems. The Direct Numerical Simulation (DNS) is the most accurate approach for simulating the turbulent flows. It solves the full Navier-Stokes equation directly using very fine mesh to capture all the scales involved in the flow. Therefore, computationally DNS would require computing power which is many orders of magnitude higher than available in the foreseeable future.

An alternative approach called Large Eddy Simulation (LES) model has developed rapidly and has wide range of applications. In LES the large length scales of the turbulent flow are computed directly and only small length scales are modelled. It can be interpreted as a low pass-filtering by time- and spatial- averaging of the Navier-Stokes equations. Since the large eddies contain most of the turbulent energy and LES captures these eddies in full detail directly whereas they are modelled in the RANS approach. LES is therefore more accurate than the RANS approach and requires less computational resources than DNS.

Therefore, LES will be used to simulate the drag and lift forces on the tube in the tube array in the present study.

4.2 Computational Domain and Mesh

The forces on the central tube in a rotated triangular tube array are predicted using CFD. Transient, three-dimensional simulations using LES turbulence model have been carried to capture the effects of Reynolds number on force coefficients. All simulations were performed on the commercial CFD software CFX.

The computational domain is a rotated triangular tube array with a pitch ratio of 1.5 as shown in Figure 4-1. There are 13 rows and 5 columns of tubes and the central tube is displaced to 1.5mm (0.068D) in the transverse direction. The other dimensions of the tube array are the same as the experimental test section except for the height which is the half of the test section to reduce the computational cost. Quasi-2D simulation (taking the height of the tube array to be very small) was not considered in this work as the preliminary results indicating that the outlet boundary affects the

lift force on the central tube significantly in 2D simulation. The outlet flow is not symmetrical but deviates to one side.

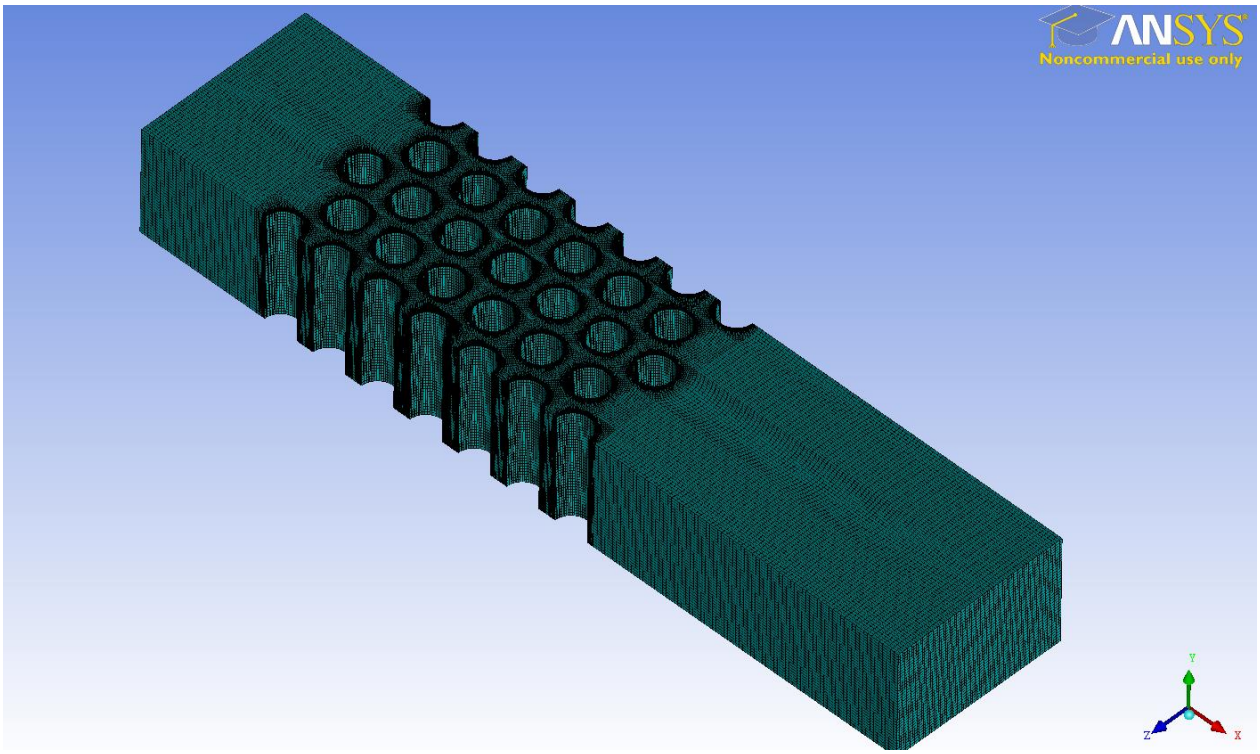

Figure 4-1 : Computation domain

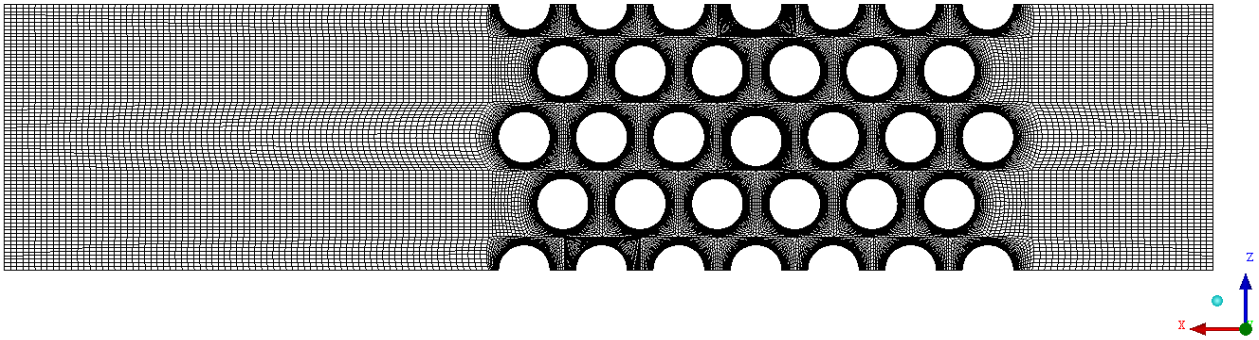

Figure 4-2 : Top view of the mesh

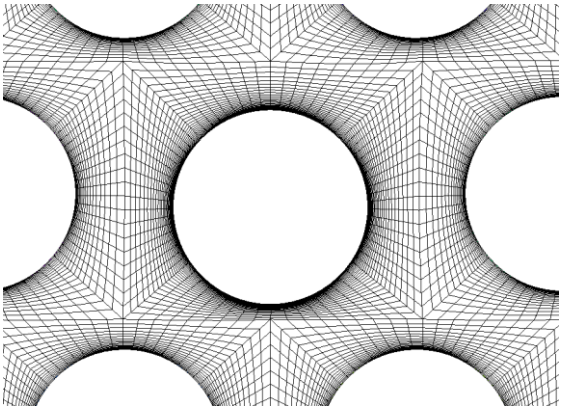

Figure 4-3 : Local mesh around the central tube

Close-up views of the top surface mesh and the central tube mesh are shown in Figure 4-2 and Figure 4-3. The mesh information is given in Table 4-1. The boundary conditions are listed in Table 4-2. Two cases, $\mathrm{Re} = 3.3\times10^4, (U_\infty = 0.5m/s)$ and $\mathrm{Re} = 9.2\times10^4, U_\infty = 1.4m/s$ were analyzed in the present work to study the effect of Reynolds number. The results are presented below.

Table 4-1 : Mesh information of the computation domain

Mesh Information		
Number of nodes		1888000
Number of Elements		1786746
Dimensions	[Min X, Max X]	[0, 0.516] [m]
	[Min Y, Max Y]	[0, 0.07] [m]
	[Min Z, Max Z]	[-0.11432, 0] [m]

Table 4-2 : Boundary condition

Boundary Condition	
Inlet	Velocity
Outlet	Average Static Pressure
Full tube and half tube	No Slip Wall
Side A and B	No Slip Wall
Top surface	Symmetry
Bottom Surface	No Slip Wall

4.3 Simulation results

Case I $\mathrm{Re} = 3.3\times10^{4}, (U_{\infty} = 0.5 m/s)$

The total simulation time is 2.8s and the time step is 0.1ms. The averaged flow field is presented in Figure 4-4 : Time averaged streamline via flow streamlines. A close-up view of the streamlines around the central tube is given in Figure 4-5 : Local streamline around the central tube. A stagnation point appears on the bottom right of the surface of tube C (central tube), while two symmetric stagnation points appear on the surface of tube F (the tube in the upstream). These stagnation points can also be seen in the pressure distribution in Figure 4-6 : The contour of averaged pressure. A comparison of the flow field around tube C and tube F shows that the symmetric flow field is disturbed by the tube displacement.

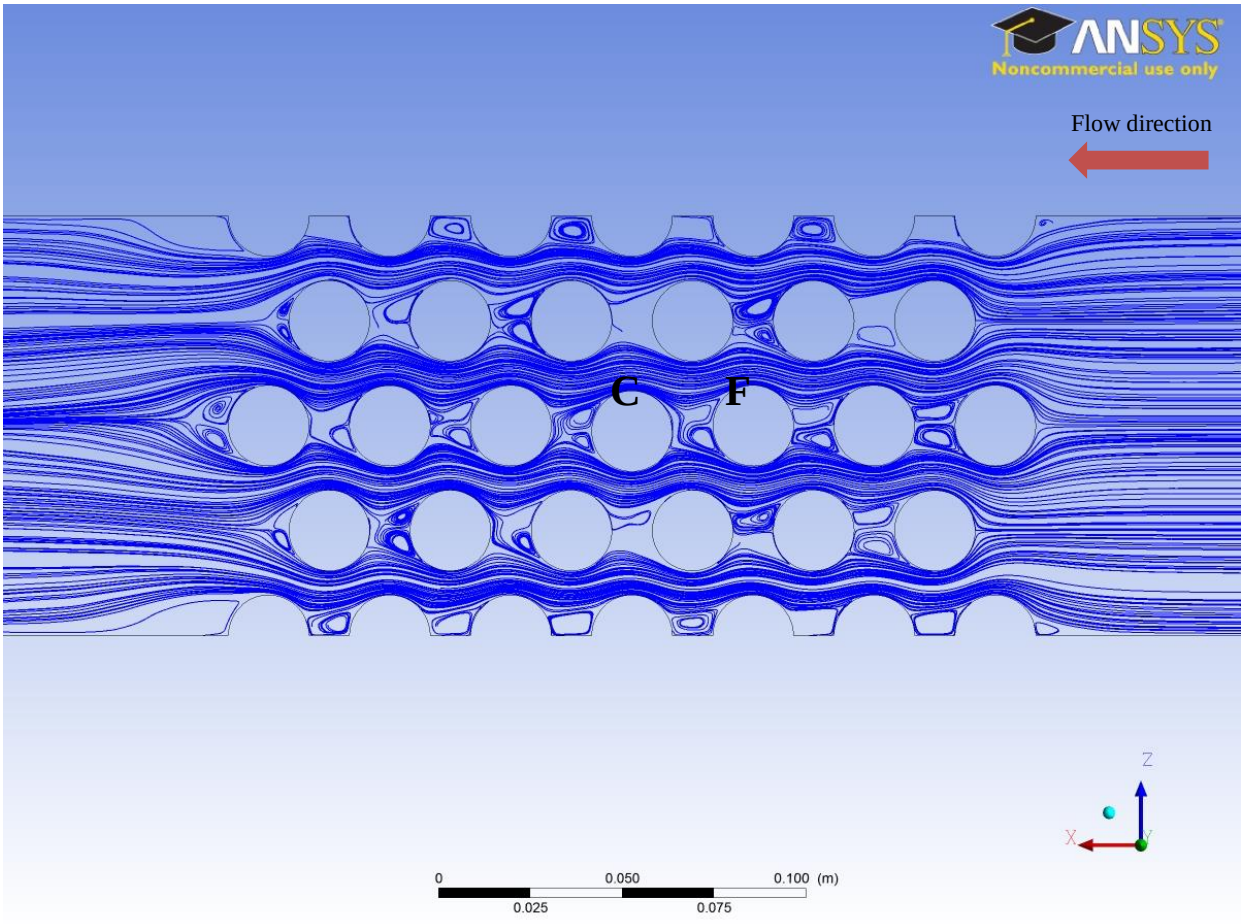

Figure 4-4 : Time averaged streamline

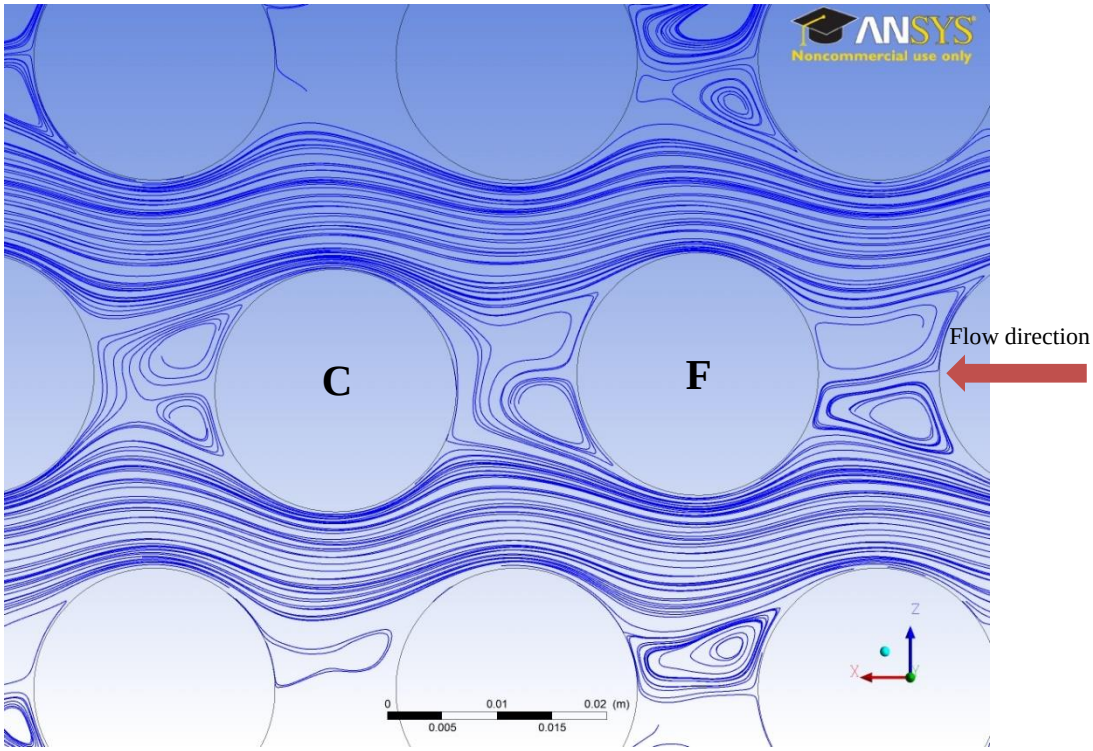

Figure 4-5 : Local streamline around the central tube

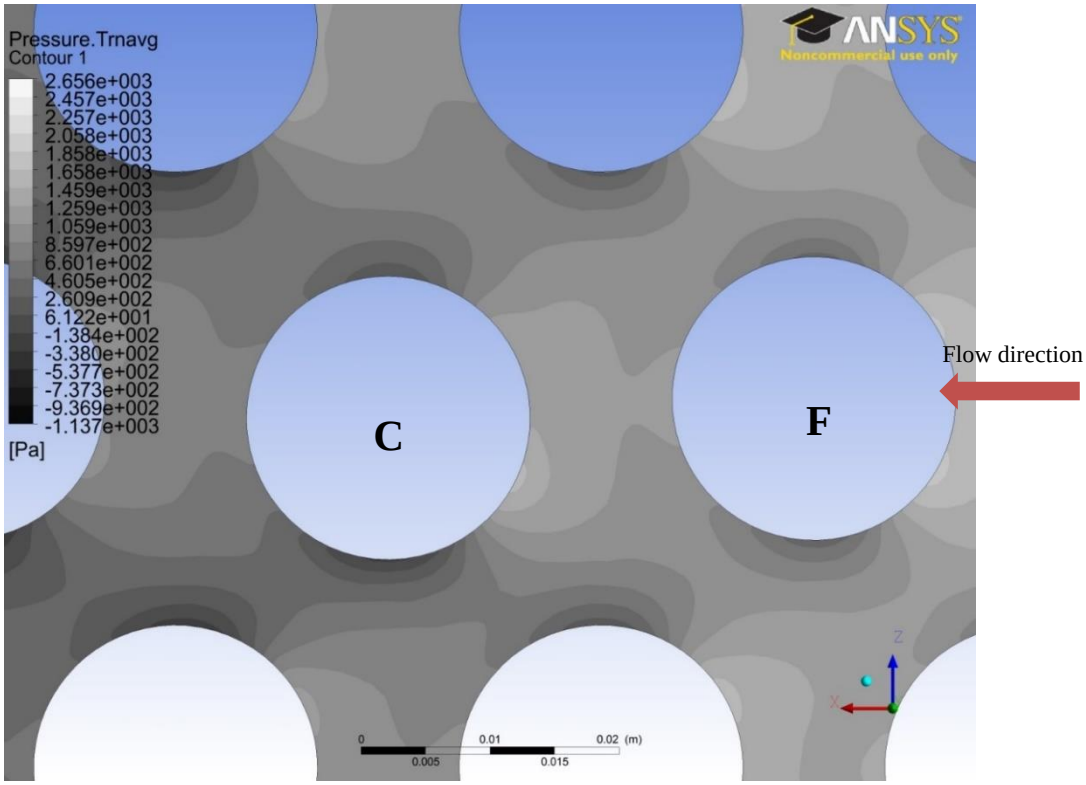

Figure 4-6 : The contour of averaged pressure

From the contours of the averaged pressure and the time-averaged streamlines, two phenomena occur due to the displacement of the central tube. (1) A stagnation point appears at the bottom right of the tube; (2) the flow velocity below the tube becomes higher than above the tube.

The stagnation point at the bottom right creates a positive lift force (normal Z direction as shown in the figure). The larger flow velocity below the tube causes a larger negative pressure region at the bottom than at the top of the tube resulting in a negative lift force. The resulting lift force is dependent on the balance between these two contributions.

In this case, with displacement 1.5mm (0.07D) and upstream flow velocity 0.5m/s, the balance between these two contributions leads to a negative resulting lift force as shown in Figure 4-7 : Drag and lift force.

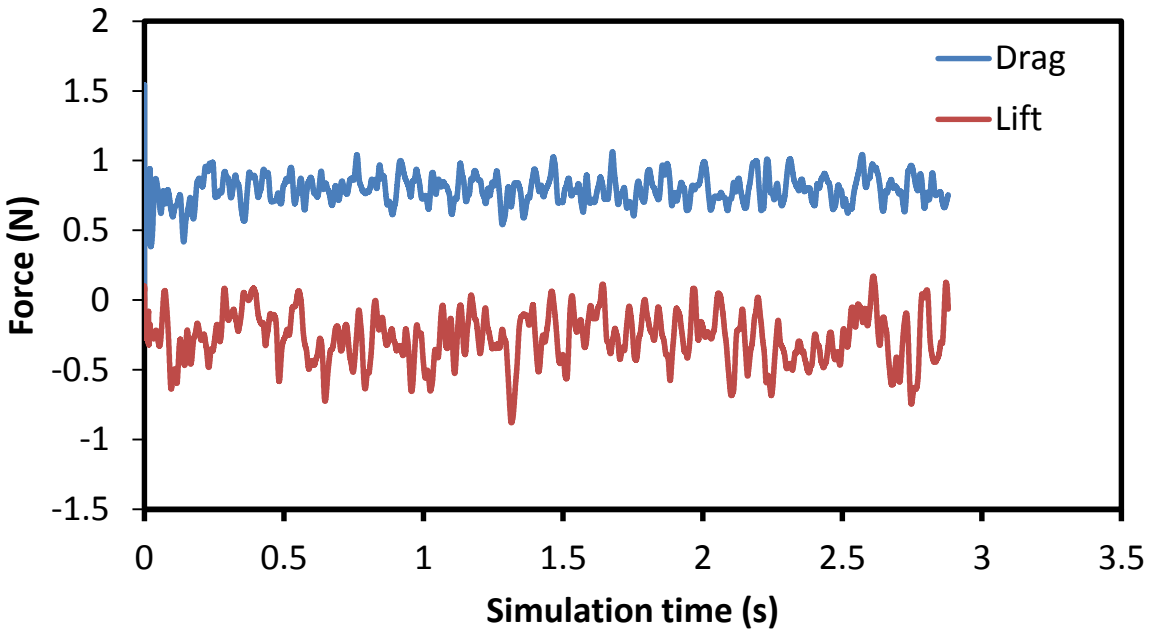

Figure 4-7 : Drag and lift force

To check if the mean flow is steady, the force data were averaged every 0.6s from 0.2s to 2.6s with a 50% overlap as shown inFigure 4-8 : Mean drag and lift forces. The mean drag and lift forces on the central tube are seen to be steady.

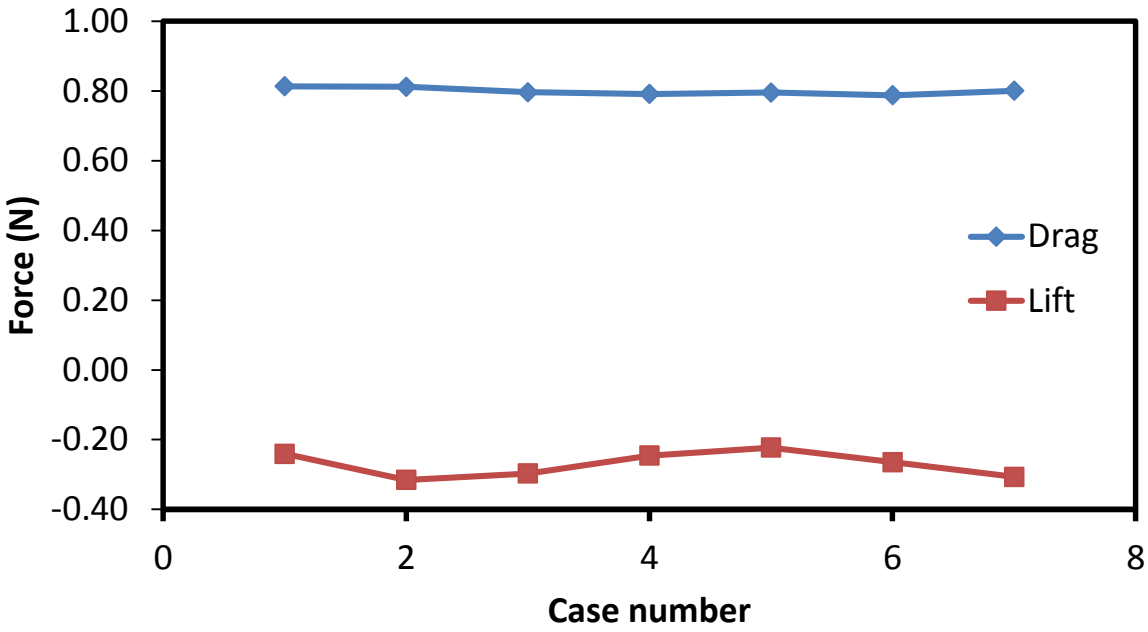

Figure 4-8 : Mean drag and lift forces

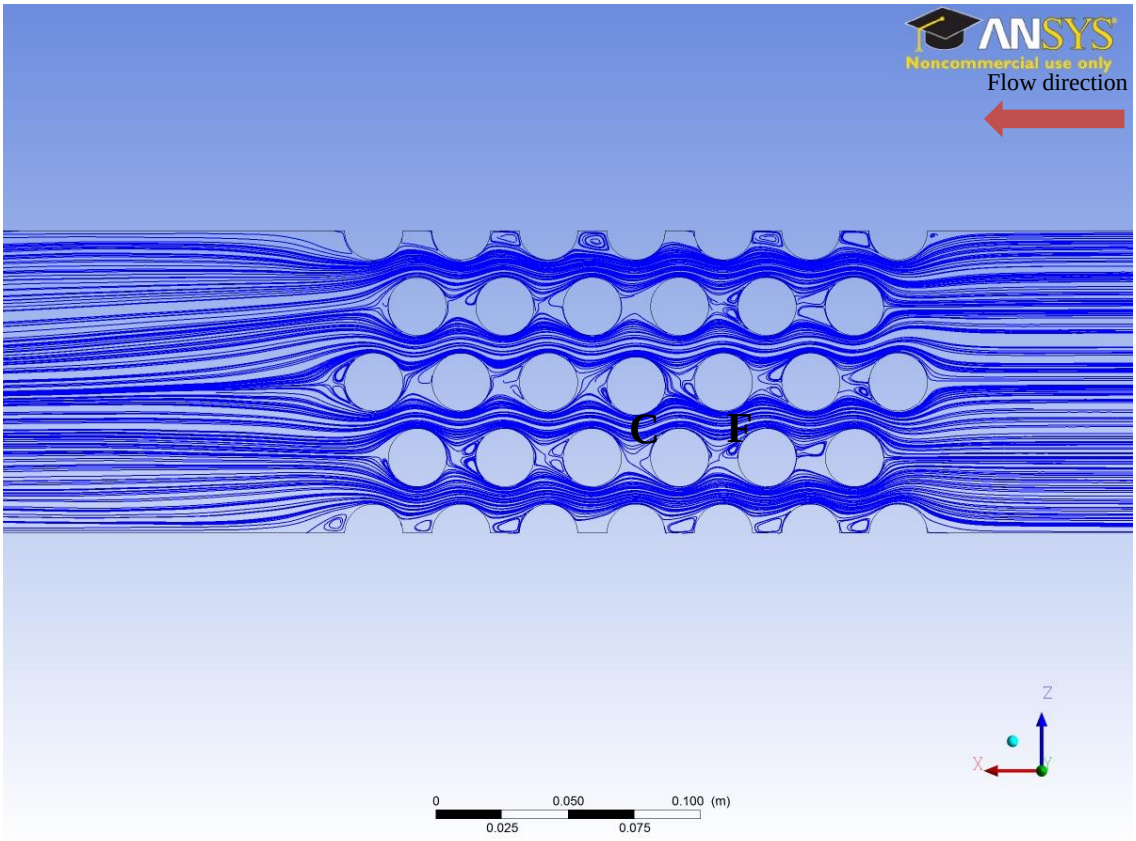

Figure 4-9 : Time averaged streamline

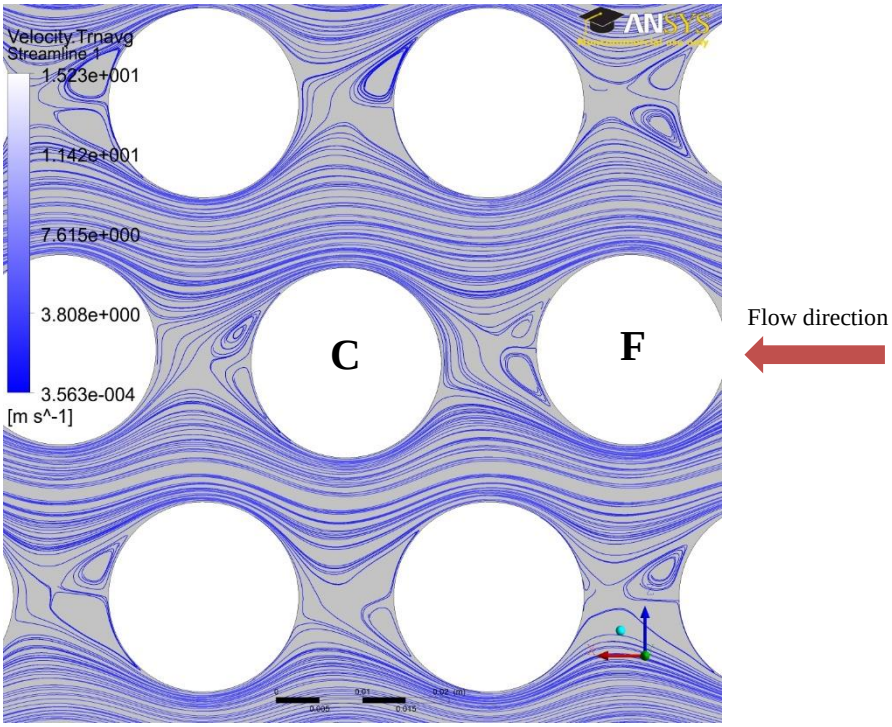

Figure 4-10 : Local streamline around the central tube

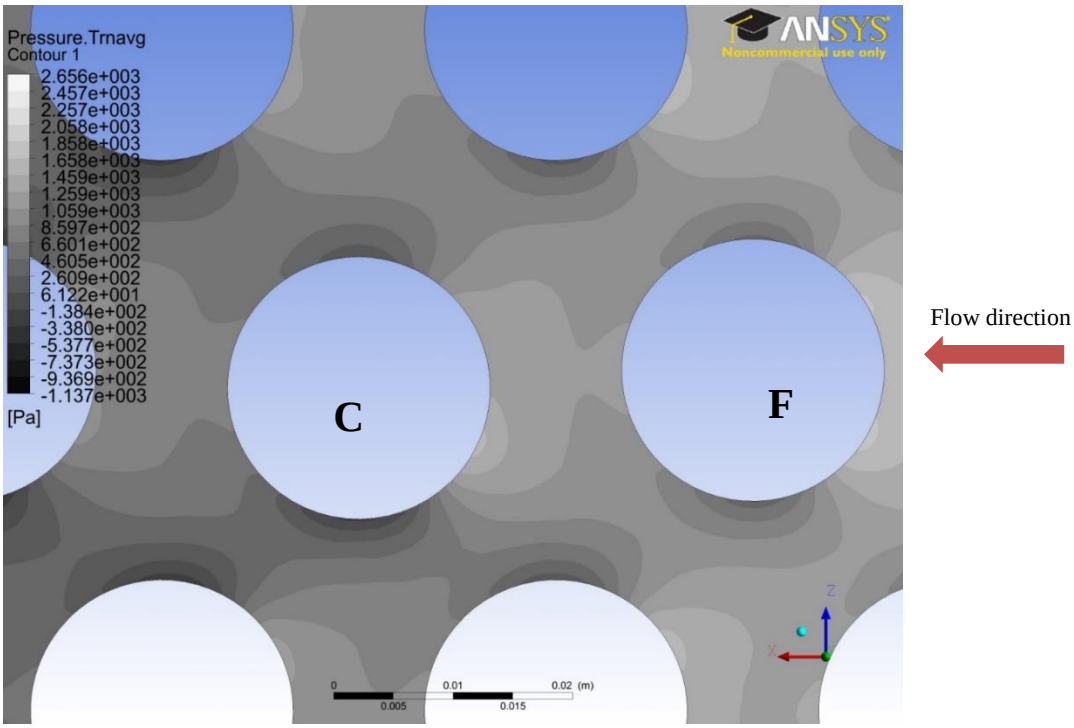

Figure 4-11 : The contour of averaged pressure

Case II $\mathrm{Re} = 9.2\times10^4, U_\infty = 1.4 m/s$

The total simulation time is 1.8s and the time step is 0.05ms in this case. The averaged flow field is presented in Figure 4-9. A close-up view of the streamlines around the central tube is given in Figure 4-10. A stagnant point appears at the bottom right of the surface of tube C, while two symmetric stagnant points appear at the surface of tube F, which is the same as the case with lower Reynolds number. This stagnant point can also be seen in the pressure distribution in Figure 4-11.

In this case, with displacement of 1.5mm (0.07D) and upstream flow velocity 1.4m/s, the balance between these two contributions leads to a negative resulting lift force as shown in Figure 4-12.

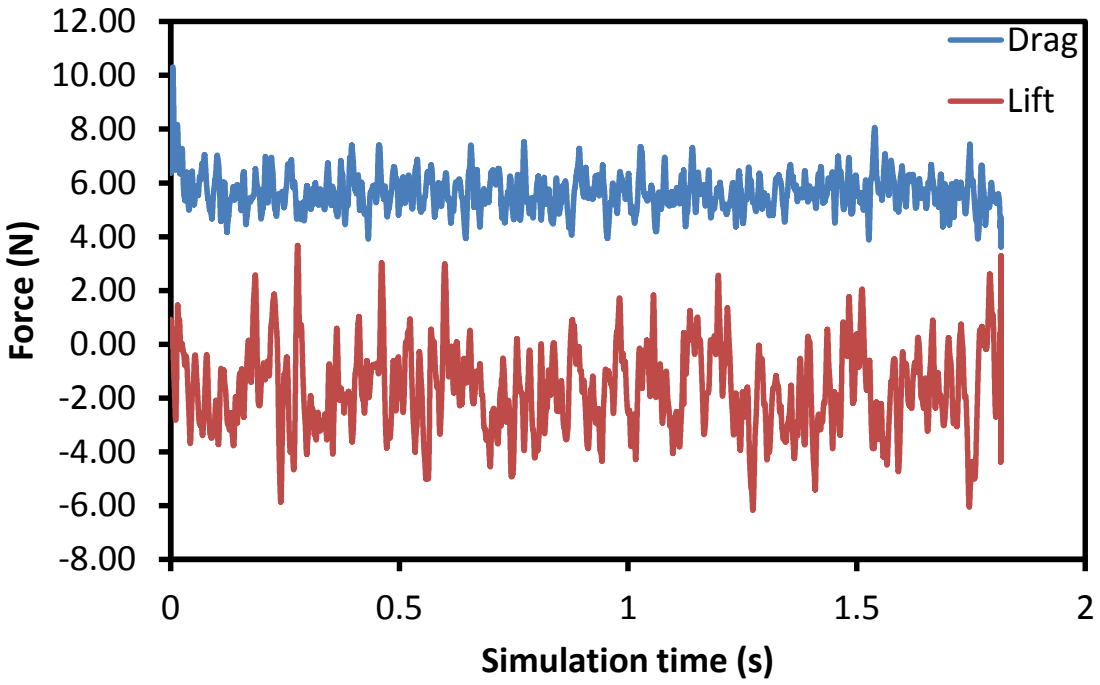

Figure 4-12 : Drag and lift force

To check if the mean flow is steady, the force data were averaged every 0.6s from 0.2s to 1.7s with a 50% overlap as shown in Figure 4-13. The mean drag and lift forces on the central tube are again seen to be steady.

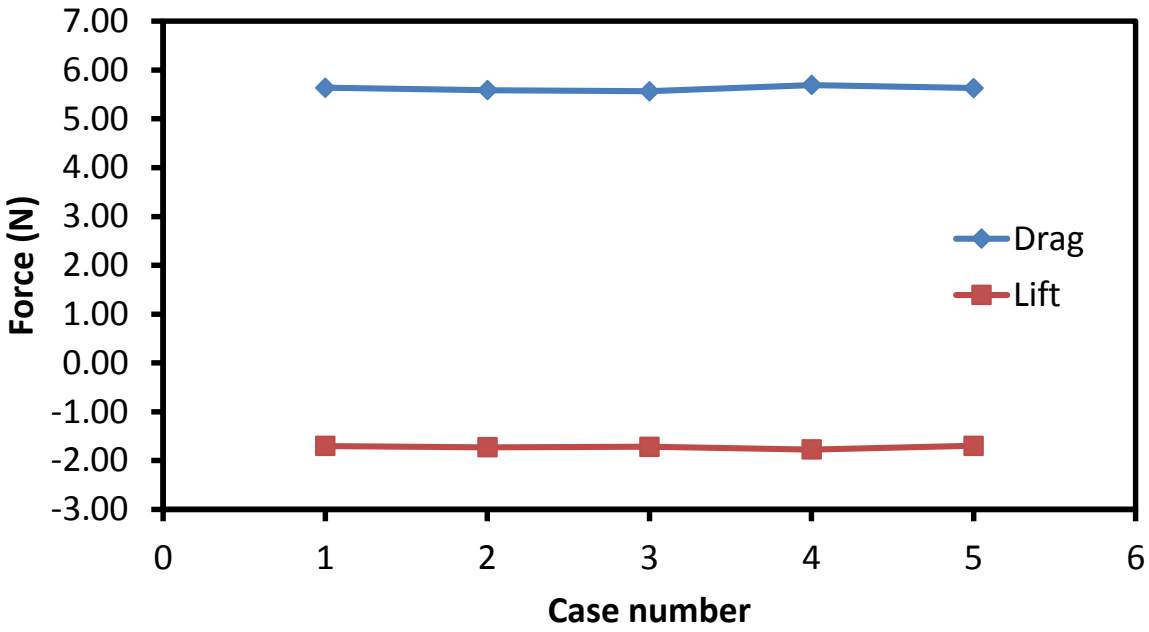

Figure 4-13 : Mean drag and lift forces

Table 4-3 : Results comparison with experimental data

	$C_{D\_\exp}$	C_{D_cfd}	$C_{L\_\exp}$	C_{L_cfd}	C_{L,y_exp}	C_{L,y_cfd}
Case I (0.5m/s)	0.39	0.46	0.02	-0.16	-0.3	2.23
Case II (1.4m/s)	0.36	0.41	-0.008	-0.13	0.11	1.86

The drag and lift coefficients are listed in Table 4-3. Note that the force coefficients are obtained based on pitch velocity. The drag coefficients obtained from CFD are slightly higher than those measured from experiments (18.5% and 16.5% for Case I and Case II, respectively). This shows a satisfactory agreement between the experiments and simulations in CFX. However, the lift coefficients obtained from CFD are questionable. For Case I, the lift coefficient obtained from CFD shows an opposite lift direction to the experiment results. The same lift direction was predicted for Case II. Both cases predicted much higher lift forces. Part of the reason may come from the different position of the central tube as the experiment was carried out on the central tube in the

11^{th} row while the central tube in the simulation is in the 7^{th} row. However, more work is clearly needed to improve the CFD analysis.

As we know that the lift force on the central tube with minor displacement is much smaller compared to the drag force, the effects of the turbulence and the boundary layer at the surface of the tube become very important. It is questionable if the computational model can catch the characteristic of the flow around the central tube, especially in the lift direction. Computations for several larger displacements are therefore needed. Although the simulation fails to give satisfactory results for the lift force on the central tube, the results of drag forces are acceptable which still gives us some confidence in the reliability of CFD. Obviously, more work is needed to close the discussion.

It should be mentioned that CFD provides us more information of the flow around the central tube in the tube array. It is clear now that the mean lift force on the central tube is dependent on two parameters. One is the position of the stagnation point and the other is the negative pressure region caused by the difference between the flow velocity at the top of the tube and the flow velocity at the bottom. The results suggest that, to clearly understand the effect of Reynolds number on the lift coefficient, it will be important to measure the detailed pressure distribution around the tube.

CHAPTER 5 GENERAL DISCUSSION

As a reminder, the main objective of this research project was to develop a time delay formulation for the class of quasi-steady fluidelastic instability models.

The results of this project were presented in the paper (Chapter 3). The unsteady aerodynamics theory was applied to cylinders in the tube array. The particular case of a single flexible tube in an otherwise rigid array was considered for simplicity. An Equivalent Theodorsen Function was applied to arrive at a time delay formulation in the frequency domain. Unsteady fluid force coefficients and quasi-static forces coefficients were measured in a rotated triangular tube array to determine the Equivalent Theodorsen Function.

It was found that the lift derivative is strongly dependent on Reynolds number which suggests that the fluidelastic instability is also dependent on Reynolds number. This Reynolds number effect was then investigated using a numerical method in ANSYS CFX. It shows that two parameters are related to the mean lift force on the central tube. One is the position of the stagnation point and the other is the negative pressure region caused by the difference between the flow velocity at the top of the tube and the flow velocity at the bottom.

The introduction of the equivalent Theodorsen equation makes it possible to take into account the effect of Reynolds number in the proposed FEI model. An initial overshoot was found in the time delay function. The overshoot has also been reported for other fluid-structure interaction systems involving bluff bodies and it is assumed to be related to the flow separation and the growth of the separation bubble.

The performance of the proposed model was evaluated by the stability analysis of a single flexible tube in an otherwise rigid array. The stability analysis shows very satisfactory agreement with the experimental results for $m\delta / \rho D^2 \leq 1$. It should be mentioned that the Equivalent Theodorsen Function proposed in this work is only applicable to damping controlled instability system (a single flexible tube). We note, however, that the Equivalent Theodorsen Function remains valid for the stiffness controlled instability system (multiple flexible tubes) with appropriate considerations.

In what follows, some supplementary discussions will be presented, including the flow periodicities in tube arrays, the general relation of time delay function for aeroelastic systems and the limitation of the stability analysis.

5.1 Flow periodicity in tube arrays

Generally, tube arrays subject to cross flow are excited by the periodic fluid forces, the frequency of which increases linearly with the flow velocity. This periodic excitation is known as: flow periodicity, Strouhal periodicity, or periodic vortex shedding. A narrow band of peak appears in the turbulence and pressure spectra as shown in Figure 5-1. This kind of excitation may amplify tube vibrations in liquid flow if the vorticity shedding frequency coincides with the tube natural frequency. This excitation reveals itself by a constant Strouhal number which depends on the tube array geometry, the pitch ratio, the Reynolds number and the location within the tube array as shown in Figure 5-2. Many experimental and numerical works have been carried out in flow around different tube array configurations, such as normal square (Oengören & Ziada, 1992; S Ziada & Oengören, 1992), rotated square (Price et al., 1995; D. Weaver et al., 1993), normal triangular (Polak & Weaver, 1995; S Ziada, 1998) and rotated triangular tube arrays (Price et al., 1995; S Ziada & Oengören, 2000).

As shown in Figure 1-1, the flow periodicity has the second highest potential for tube array instability. Although the flow periodicity excitation seems impossible to occur in the rotated triangular tube array with small pitch ratio and cross-flow at high Reynolds number in the present work, ensuring that periodic vortex shedding is not significant in the FEI region a pre-requisite for fluidelastic instability modeling.

The power spectral density (PSD) of the measured static fluid forces acting on the central tube is plotted in Figure 5-3. No clear peak appears in the spectra that can be attributed to periodic flow activities. The background turbulence level increases gradually as the flow velocity increases. It is expected as the central tube is in the 11^{th} row, the pitch ratio is 1.5 and the Reynolds number is high. The flow periodicity is weakened by the high turbulence of the flow. The possibility of the flow periodicity excitation is, therefore, ruled out in this work.

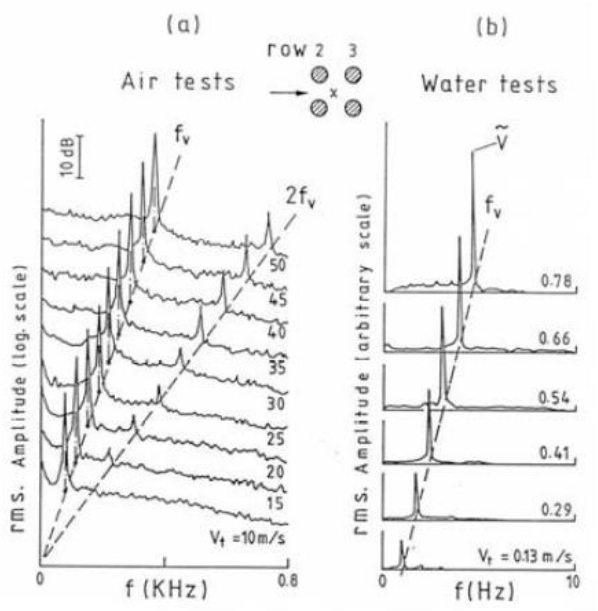

Figure 5-1 : Typical fluctuating velocity spectra of an in-line tube bundle. (a) air tests; (b) water tests. (Samir Ziada, 2006)

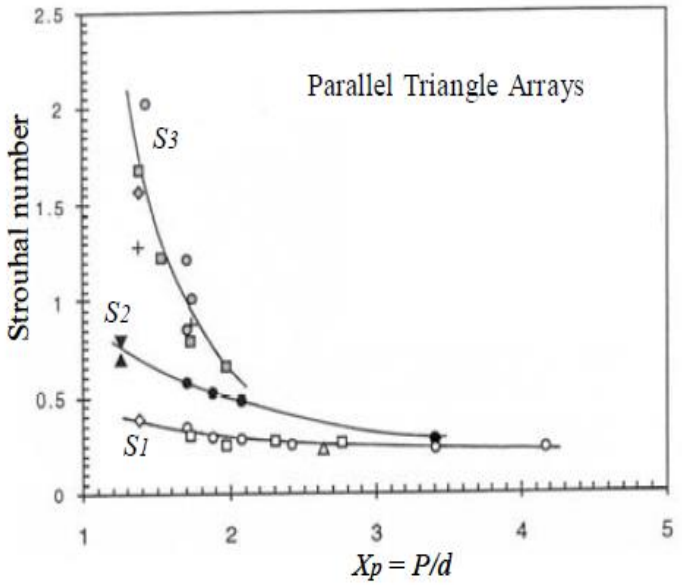

Figure 5-2 : Typical Strouhal number chart for vorticity shedding in parallel triangle arrays.

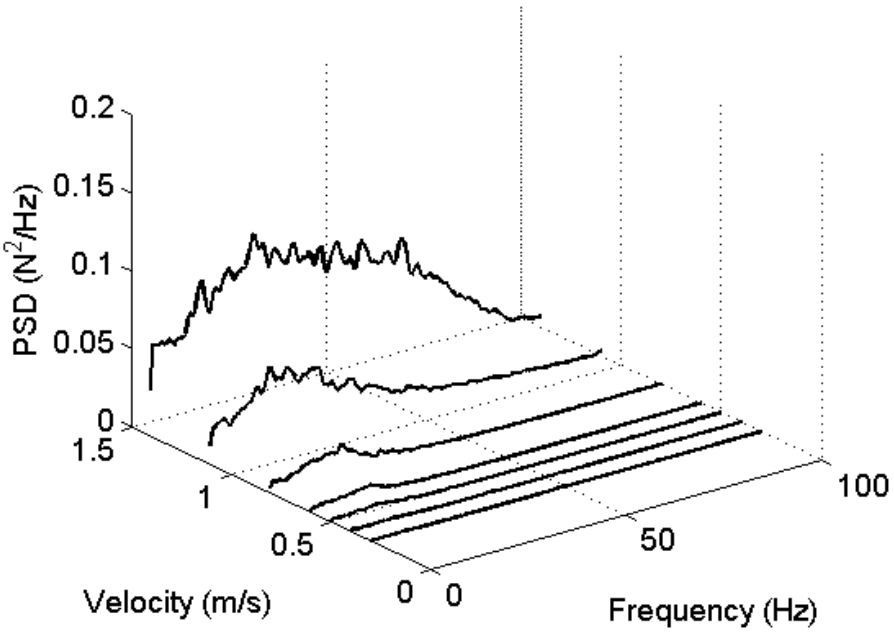

Figure 5-3 : PSD of the static fluid forces acting on the central tube in the rotated triangular tube array versus velocity.

5.2 General relation of time delay function with aeroelastic system

Generally, the flow-induced forces acting on an object placed in a cross-flow will be time-dependent due to the object motion, the flow turbulence or the vortex shedding effect. In other words, the flow-induced forces can be classified as movement-induced forces, turbulent-induced forces and vortex-induced forces. Based on the analytical movement-induced forces, many theoretical models have been proposed for the purpose of structural stability analysis and design. In these models, the time delay effect, which may greatly affects the structure characteristics, should be considered carefully.

This time delay effect on flow-induced forces has been studied in different research fields, especially in the aerodynamics theory of airfoils and bridge decks and also in the fluidelastic instability theory of tube arrays. In this section, the relation of the time delay effects among these theories will be discussed.As noted before, the time delay effect on the unsteady aerodynamic forces acting on the airfoils can be described in both time- and frequency-domains. In the time domain, the most famous time delay effect was proposed by Wagner (1925). When a sudden step change of the attack angle of the airfoil is considered, the lift force undergoes a transient change

described by the time delay effect which is called the indicial function. The indicial function was determined theoretically for thin airfoils in the potential flow and is shown in Figure 2-8. It is seen that half of the final lift is assumed before the airfoil experiences the step change and then approaches asymptotically its steady lift when the non-dimensional time $\tau \to \infty$.

With regard to the frequency domain, Theodorsen obtained the time delay effect by considering the airfoil undergoes a harmonic motion. Although the lift force is expressed in the time domain, the time delay effect (the Theodorsen function) is defined in the frequency domain which is the built-in characteristic of the classical flutter theory. The function was originally expressed in terms of modified Bessel or Hankel functions. The real and imaginary parts of the function are $F(k)$ and $G(k)$, which are shown in Figure 2-9. It is noteworthy that the Theodorsen and Wagner functions are equivalent representation of the time delay effect in the frequency and the time domains, respectively.

These two classical models described in both time and frequency domain still remain widely used today and are also extended to the motion-induced forces on bluff bodies such as bridge decks and rectangular cylinders. It is important to note that the classical Wagner and Theodorsen models were developed based on the potential flow theory. Hence this form does not hold for bluff objects for which flow separation typically occurs. Instead of proposing the analytical force model analogous to the two classical models, it is common practice to obtain frequency-dependent functions (namely, the flutter derivatives or aeroelastic derivatives which are similar to the Theodorsen function) for bluff bodies by experimental methods. On the other hand, an indicial function which described the time delay effect, or to be more specific the force response to the step change of the bridge deck in the time domain, can be determined from the flutter derivatives. A typical indicial function is plotted in Figure 5-4, wherein, the behavior of the time delay effect is very different from the classical indicial function of an airfoil. There is a significant overshoot in the response compared to Figure 2-8. Instead of approaching the steady lift asymptotically, it overshoots at the beginning and then decreases to the steady value. This phenomenon has been studies by many researchers (Hatanaka & Tanaka, 2008; R. Scanlan, 2000; Turbelin & Gibert, 2002). The results to date suggest that the overshoot is related to the growth of separation bubbles from the leading edges.

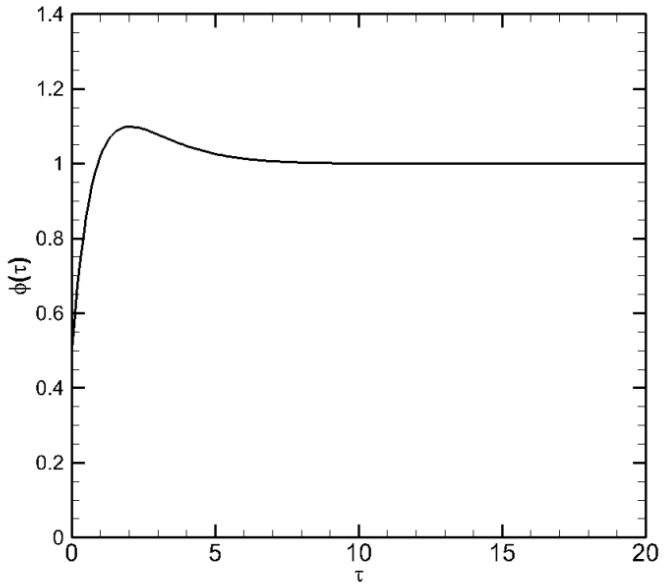

Figure 5-4 : Typical indicial function of a bluff body

The time delay effect in the fluidelastic instability models for tube arrays has also been studied by many researchers such as the quasi-steady model (1984) and the quasi-unsteady model (1996). The typical memory functions as well as the memory function derived from the Equivalent Theodorsen Function in this work are depicted in Figure 3-14. In the quasi-steady model, the time delay effect was modelled as a step function at $\tau = \mu$. As the tube experiences a step change of the position, the flow will retain the steady state for $\tau < \mu$ and achieve instantaneously a new steady state at $\tau = \mu$. This behavior is clearly physically unrealistic. Unlike the constant time delay effect, a continuous evolution of the flow is considered in the quasi-unsteady model. The step response behaves similarly to that for an airfoil which approaches asymptotically its steady lift as $\tau \to \infty$. While for the current model, derived from the Equivalent Theodorsen Function, a strong overshoot occurs in the memory function which is similar to the typical behavior of other bluff bodies. Given the generality in the aerodynamics and fluid dynamic theories of airfoils, bluff bodies and tube arrays, it is reasonable to believe that it is the same fundamental phenomenon in the flow (separation bubble) that causes the overshoot in the memory function in tube arrays. The flow separation point position and the vortex size may be affected by the Reynolds number which causes the different strengths of the overshoot.

The first-order memory function of the quasi-unsteady model is a kind of a low-pass first-order filter. The parameters were obtained empirically by just one measurement at which fluidelastic instability occurs in the dynamic tests. It is, indeed, a practical way to extract the parameters and then use them to predict the critical velocity. However, it may filter some of the transient behaviors of the motion-induced forces, such as the overshoot in the memory function.

To recap, the time delay which characterizes the motion-induced forces has a significant effect on the system stability in the aerodynamics theories of airfoils and bluff bodies and in the fluidelastic instability models of tube arrays. Although the expressions of the memory function may differ from each other due to the different structures and flow fields, the underlying principle is identical. The main difference is the method employed to determine the memory functions. The classical Wagner and Theodorsen models of aerodynamics theories for airfoils were developed based on potential flow theory while the memory functions of bluff bodies and tubes in tube arrays have been obtained by experimental means.

5.3 Limitation of the stability analysis

A stability analysis of a single flexible tube in an otherwise rigid array was carried out to validate the performance of the Equivalent Theodorsen Function. The method and results are presented in Section 3.4.4.

It is well known that the lift derivative is important for FEI model. The lift derivative is usually assumed to be constant at high Reynolds number, while the experiment in the present work shows that it strongly depends on Reynolds number which makes the FEI model more complicated. The results imply that FEI may be strongly dependent on Reynolds number. In the present work, all the force measurements were conducted for $\mathrm{Re} \le 9.2\times10^4$ due to the limitation of the test loop. In the stability analysis, the mass damping parameter for water flow is therefore limited to $m\delta / \rho D^2 \le 1$ as shown in Figure 3-15.

The lift derivative is found to decrease quasi-linearly with increasing Reynolds number but the trend changes and the derivative becomes positive at high Reynolds number. It would be interesting to know if the relation is valid for any Re, and what kind of the instability threshold the proposed FEI model can predict. The stability threshold is plotted in Figure 5-5. The model gives very satisfactory agreement with experiments for lower mass damping parameter in the range where the

model is valid. Although it shows the right trend for the threshold, it underestimates the critical velocity for higher mass damping parameter and fails to predict instability for $m\delta/\rho D^2 \geq 3$. This may be due to the limitation of the damping controlled FEI model. It is generally agreed that FEI is caused by the damping controlled mechanism at lower mass damping parameter $m\delta/\rho D^2 \leq 1$ and by stiffness controlled mechanism at higher mass damping parameter. As noted earlier, consideration in the present work is only given to a single flexible tube in an otherwise rigid array for simplicity. The model can therefore only predict damping controlled instability. Nevertheless, the results certainly give some confidence in the reliability of the method and suggest that further work on time delay of multiple flexible tubes would be useful.

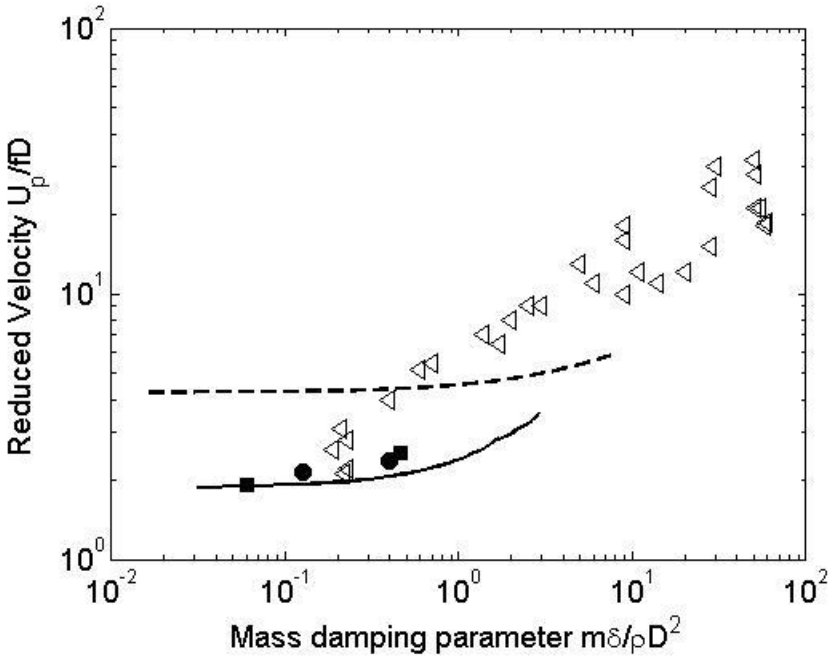

Figure 5-5 : Stability threshold for rotated triangular tube arrays. ◁, experiment data from (D. t. Weaver & Fitzpatrick, 1988); ■, experiment data from (Sawadogo & Mureithi, 2014b); ●, experiment data from (Violette et al., 2006); −− , Quasi-unsteady model; − , Current model

CHAPTER 6 CONCLUSION AND RECOMMENDATIONS

6.1 Conclusions

A new time delay formulation for the class of quasi-steady fluidelastic instability models has been proposed in this Master's project. The main conclusions drawn from the present work are as follows:

- A time delay formulation was derived in the form of an Equivalent Theodorsen Function.
- Measure and study in detail the unsteady and the quasi-static fluid forces in a rotated triangular tube array subjected to water flow. The time delay formulation was then determined using the measured fluid force coefficients.
- The time delay formulation was compared with other time delay functions found in the quasi-steady and quasi-unsteady models. An initial overshoot in the lift force was observed for the present model. The overshoot has also been reported for other fluid-structure interaction problems involving bluff bodies.
- The time delay was found to be dependent on Reynolds number which implies that the fluidelastic instability is also Reynolds number dependent. The present FEI model with the Equivalent Theodorsen Function makes it possible to conveniently take into account the effect of Reynolds number.
- A stability analysis using the new time delay formulation was presented and compared to the quasi-steady and quasi-unsteady models as well as experimental data. The predicted stability threshold compares reasonably well with experimental data and shows a significant improvement over the other models.
- The foregoing stability analysis results confirm the validity of the model and give some confidence in the reliability of the method. The reader is reminded that the time delay formulation is obtained from experiments on a rotated triangular tube array with a pitch ratio of 1.5 subjected to single-phase cross-flow. The Equivalent Theodorsen Function correlation obtained is therefore only applicable to the rotated triangular tube array and valid for the range of Re considered. However, the method itself is more generally applicable to the other tube arrays.

6.2 Limitations and challenges

The lift derivative, which is important to the proposed FEI model, is sensitive to Reynolds number. The limited capacity of the pump used in the experiments did not allow measurements of the lift derivative for higher Reynolds number. The sign of the lift derivative changes from negative to positive at around $\mathrm{Re} = 8 \times 10^4$ and the reason for the change is not well understood yet. Further study is therefore required to clarify this point.

This study is limited to the lift direction of a rotated triangular tube array subjected to water cross-flow. Due to the fact that the fluidelastic instability in this condition is dominated by the damping controlled mechanism, the proposed model fails to predict the critical velocity at higher mass damping parameter where the instability is dominated by stiffness controlled mechanism. It is desirable to extend the time delay formulation, developed here for the lift direction, to the drag direction.

Finally, the tube arrays in steam generators operated in two-phase flow condition. The nature of two-phase flow, such as higher turbulence level, void fraction uncertainty and possible flow regime transition, makes the problem more complicated. It is, however, interesting and useful for further investigation to see if the proposed FEI model can apply to two-phase flows.

6.3 Recommendations

1. Increase the capacity of the water pump in order to measure the lift derivative at high Reynolds number. Install some pressure taps on the surface of the central tube in order to measure the fluid forces and obtain more information about the flow around the tube.
2. Adapt the proposed FEI model to the tube array with multiple flexible tubes.
3. Extend the proposed FEI model from water flow to two-phase flow.
4. Consider the effect of different tube array configurations and pitch-to-diameter ratios.

BIBLIOGRAPHY

Blevins, R. D. (1974). Fluidelastic whirling of a tube row. *Journal of Pressure Vessel Technology*, 263-267.

Braun, A. L., & Awruch, A. M. (2003). Numerical simulation of the wind action on a long-span bridge deck. *Journal of the Brazilian Society of Mechanical Sciences and Engineering, 25*(4), 352-363.

Charreton, C., Béguin, C., Yu, K., & Étienne, S. (2015). Effect of Reynolds number on the stability of a single flexible tube predicted by the quasi-steady model in tube bundles. *Journal of Fluids and Structures, 56*, 107-123.

Chen, S. (1984). Guidelines for the instability flow velocity of tube arrays in crossflow. *Journal of Sound and Vibration, 93*(3), 439-455.

Chen, S. (1987). A general theory for dynamic instability of tube arrays in crossflow. *Journal of Fluids and Structures, 1*(1), 35-53.

Chen, S., & Jendrzejczyk, J. (1983). Stability of tube arrays in crossflow. *Nuclear Engineering and Design, 75*(3), 351-373.

Connors. (1970). Fluidelastic vibration of tube arrays excited by cross flow. *ASME Winter Annual Meeting*, pp. 42–56.

Connors, H. (1978). Fluidelastic vibration of heat exchanger tube arrays. *Journal of Mechanical Design, 100*(2), 347-353.

Farsani, H. Y., Valentine, D. T., Arena, A., Lacarbonara, W., & Marzocca, P. (2014). Indicial functions in the aeroelasticity of bridge decks. *Journal of Fluids and Structures, 48*, 203-215.

Fung, Y.-c. (2002). *An introduction to the theory of aeroelasticity*: Courier Corporation.

Garrick, I. E. (1938). On some reciprocal relations in the theory of nonstationary flows.

Gorman, D. (1976). Experimental development of design criteria to limit liquid cross-flow-induced vibration in nuclear reactor heat exchange equipment. *Nuclear Science and Engineering, 61*(3), 324-336.

Granger, S., & Paidoussis, M. (1996). An improvement to the quasi-steady model with application to cross-flow-induced vibration of tube arrays. *Journal of Fluid Mechanics, 320*, 163-184.

Hassan, M., & Weaver, D. S. (2016). Modeling of Streamwise and Transverse Fluidelastic Instability in Tube Arrays. *Journal of Pressure Vessel Technology, 138*(5), 051304.

Hatanaka, A., & Tanaka, H. (2008). Aerodynamic admittance functions of rectangular cylinders. *Journal of Wind Engineering and Industrial Aerodynamics, 96*(6), 945-953.

Hartlen, R. (1974). *Wind-tunnel Determination of Fluid-elastic-vibration Thresholds for Typical Het-exchanger Tube Pattens*: Ontario Hydro Research Division.

Heilker, W., & Vincent, R. (1981). Vibration in nuclear heat exchangers due to liquid and two-phase flow. *Journal of Engineering for power, 103*(2), 358-366.

IAEA. (2013). IAEA annual report 2013.

Jones, R. T. (1938). Operational treatment of the nonuniform-lift theory in airplane dynamics.

Kassera, V., & Strohmeier, K. (1997). Simulation of tube bundle vibrations induced by cross-flow. *Journal of Fluids and Structures, 11*(8), 909-928.

Khalifa, A., Weaver, D., & Ziada, S. (2013). Modeling of the phase lag causing fluidelastic instability in a parallel triangular tube array. *Journal of Fluids and Structures, 43*, 371-384.

Khalvatti, A. (2007). *Effect of preferential flexibility angle on fluidelastic instability of a rotated trianglar tube bundle.* Thesis Master, École Polytechnique de Montréal.

Lever, J., & Weaver, D. (1982). A theoretical model for fluid-elastic instability in heat exchanger tube bundles. *Journal of Pressure Vessel Technology, 104*(3), 147-158.

Lever, J., & Weaver, D. (1986). On the stability of heat exchanger tube bundles, part i: Modified theoretical model. *Journal of Sound and Vibration, 107*(3), 375-392.

Luo, S., & Bearman, P. (1990). Predictions of fluctuating lift on a transversely oscillating square-section cylinder. *Journal of Fluids and Structures, 4*(2), 219-228.

Mahon, J., & Meskell, C. (2012). Surface pressure survey in a parallel triangular tube array. *Journal of Fluids and Structures, 34*, 123-137.

Meskell, C. (2009). A new model for damping controlled fluidelastic instability in heat exchanger tube arrays. *Proceedings of the Institution of Mechanical Engineers, Part A: Journal of Power and Energy, 223*(4), 361-368.

Miranda，S, D. (2013). Indicial functions and flutter derivatives: A generalized approach to the motion-related wind loads. *Journal of Fluids and Structures, 42*, 466-487.

Oengören, A., & Ziada, S. (1992). Vorticity shedding and acoustic resonance in an in-line tube bundle part II: Acoustic Resonance. *Journal of Fluids and Structures, 6*(3), 293IN3303IN5307-302306309.

Paidoussis, M. (1983). A review of flow-induced vibrations in reactors and reactor components. *Nuclear Engineering and Design, 74*(1), 31-60.

Pettigrew, M., Sylvestre, Y., & Campagna, A. (1978). Vibration analysis of heat exchanger and steam generator designs. *Nuclear Engineering and Design, 48*(1), 97-115.

Pettigrew, M., & Taylor, C. (1991). Fluidelastic instability of heat exchanger tube bundles: review and design recommendations. *Journal of Pressure Vessel Technology, 113*(2), 242-256.

Pettigrew, M., & Taylor, C. (2003a). Vibration analysis of shell-and-tube heat exchangers: an overview—Part 1: flow, damping, fluidelastic instability. *Journal of Fluids and Structures, 18*(5), 469-483.

Pettigrew, M., & Taylor, C. (2003b). Vibration analysis of shell-and-tube heat exchangers: an overview—Part 2: vibration response, fretting-wear, guidelines. *Journal of Fluids and Structures, 18*(5), 485-500.

Pettigrew, M., Zhang, C., Mureithi, N., & Pamfil, D. (2004). *Detailed flow measurements in a rotated triangular tube bundle subjected to two-phase cross flow.* Paper presented at the Proceedings of the 8. international conference on Flow-induced vibration.

Polak, D., & Weaver, D. (1995). Vortex shedding in normal triangular tube arrays. *Journal of Fluids and Structures, 9*(1), 1-17.

Price, S. (1995). A review of theoretical models for fluidelastic instability of cylinder arrays in cross-flow. *Journal of Fluids and Structures, 9*(5), 463-518.

Price, S., Païdoussis, M., & Mark, B. (1995). Flow visualization of the interstitial cross-flow through parallel triangular and rotated square arrays of cylinders. *Journal of Sound and Vibration, 181*(1), 85-98.

Price, S., & Paidoussis, M. (1984). An improved mathematical model for the stability of cylinder rows subject to cross-flow. *Journal of Sound and Vibration, 97*(4), 615-640.

Price, S., & Paidoussis, M. (1986). A single-flexible-cylinder analysis for the fluidelastic instability of an array of flexible cylinders in cross-flow. *Journal of Fluids Engineering, 108*(2), 193-199.

Sawadogo, T., & Mureithi, N. (2014a). Fluidelastic instability study in a rotated triangular tube array subject to two-phase cross-flow. Part I: Fluid force measurements and time delay extraction. *Journal of Fluids and Structures, 49*, 1-15.

Sawadogo, T., & Mureithi, N. (2014b). Fluidelastic instability study on a rotated triangular tube array subject to two-phase cross-flow. Part II: Experimental tests and comparison with theoretical results. *Journal of Fluids and Structures, 49*, 16-28.

Scanlan, R. (2000). Motion-related body-force functions in two-dimensional low-speed flow. *Journal of Fluids and Structures, 14*(1), 49-63.

Scanlan, R., & Jones, N. (1999). A form of aerodynamic admittance for use in bridge aeroelastic analysis. *Journal of Fluids and Structures, 13*(7), 1017-1027.

Scanlan, R. H. (1996). Aerodynamics of cable-supported bridges. *Journal of Constructional Steel Research, 39*(1), 51-68.

Schröder, K., & Gelbe, H. (1999). Two-and three-dimensional CFD-simulation of flow-induced vibration excitation in tube bundles. *Chemical Engineering and Processing: Process Intensification, 38*(4), 621-629.

Simiu, E., & Scanlan, R. H. (1996). *Wind effects on structures*: Wiley.

Simpson, A., & Flower, J. (1977). An improved mathematical model for the aerodynamic forces on tandem cylinders in motion with aeroelastic applications. *Journal of Sound and Vibration, 51*(2), 183-217.

Soper, B. (1983). The effect of tube layout on the fluid-elastic instability of tube bundles in crossflow. *Journal of heat transfer, 105*(4), 744-750.

Tanaka, H., & Takahara, S. (1980). *Unsteady fluid dynamic force on tube bundle and its dynamic effect on vibration.* Paper presented at the ASME century 2 emerging technology conference.

Tanaka, H., & Takahara, S. (1981). Fluid elastic vibration of tube array in cross flow. *Journal of Sound and Vibration, 77*(1), 19-37.

Tanaka, H., Takahara, S., & Ohta, K. (1982). Flow-induced vibration of tube arrays with various pitch-to-diameter ratios. *Journal of Pressure Vessel Technology, 104*(3), 168-174.

Theodorsen. (1949). General theory of aerdynamic instability and the mechanism of flutter: Labgley Memorial Aeronautical Laboratory.

Turbelin, G., & Gibert, R. J. (2002). CFD calculations of indicial lift responses for bluff bodies. *Wind and Structures, 5*(2_3_4), 245-256.

Violette, R., Pettigrew, M., & Mureithi, N. (2006). Fluidelastic instability of an array of tubes preferentially flexible in the flow direction subjected to two-phase cross flow. *Journal of Pressure Vessel Technology, 128*(1), 148-159.

Wagner, H. (1925). Über die Entstehung des dynamischen Auftriebes von Tragflügeln. *ZAMM - Journal of Applied Mathematics and Mechanics/Zeitschrift für Angewandte Mathematik und Mechanik, 5*(1), 17-35.

Weaver, D.S, Lian, H., & Huang, X. (1993). Vortex shedding in rotated square arrays. *Journal of Fluids and Structures, 7*(2), 107-121.

Weaver, D.S., & Fitzpatrick, J. (1988). A review of cross-flow induced vibrations in heat exchanger tube arrays. *Journal of Fluids and Structures, 2*(1), 73-93.

Weaver, D.S, & El-Kashlan, M. (1981). The effect of damping and mass ratio on the stability of a tube bank. *Journal of Sound and Vibration, 76*(2), 283-294.

Weaver, D.S, & Grover, L. (1978). Cross-flow induced vibrations in a tube bank—turbulent buffeting and fluid elastic instability. *Journal of Sound and Vibration, 59*(2), 277-294.

Yetisir, M., & Weaver, D. (1993). An unsteady theory for fluidelastic instability in an array of flexible tubes in cross-flow. Part I: theory. *Journal of Fluids and Structures, 7*(7), 751-766.

Ziada, S. (1998). An in-depth study of vortex shedding, acoustic resonance and turbulent forces in normal triangle tube arrays. *Journal of Fluids and Structures, 12*(6), 717-758.

Ziada, S. (2006). Vorticity shedding and acoustic resonance in tube bundles. *Journal of the Brazilian Society of Mechanical Sciences and Engineering, 28*, 186-189.

Ziada, S., & Oengören, A. (1992). Vorticity shedding and acoustic resonance in an in-line tube bundle part I: Vorticity shedding. *Journal of Fluids and Structures, 6*(3), 271-292.

Ziada, S., & Oengören, A. (2000). Flow periodicity and acoustic resonance in parallel triangle tube bundles. *Journal of Fluids and Structures, 14*(2), 197-219.